MODELED RISK OF RADIATION INDUCED CANCERS AFTER PROSTATE CANCER RADIATION TREATMENT

This thesis is submitted to the University of Ghana, Legon

BY

RITA OSAFO-AYE

(10550969)

In partial fulfilment of the requirement for the award of:

MPHIL Medical Physics degree

JULY, 2017

DECLARATION

This thesis work is the results of research work undertaken by Rita Osafo-Aye in the Department of Medical Physics, School of Nuclear and Allied Sciences, University of Ghana. The research was done under the supervision of Prof. Cyril Schandorf, Dr. Stephen Inkoom and Mr. George Felix Acquah.

I hereby affirm that this thesis is the result of my own original research and that no part of it has been presented for another degree in this university or elsewhere, except where due acknowledgement has been made to the next.

……	…….
RITA OSAFO-AYE	PROF. CYRIL SCHANDORF
(STUDENT)	(PRINCIPAL SUPERVISOR)
Date……	Date……..
……...	……..
DR. STEPHEN INKOOM	MR. GEORGE FELIX ACQUAH
(CO-SUPERVISOR)	(CO-SUPERVISOR)
Date…….	Date……

ABSTRACT

This study investigates into the second cancer risks to the bladder and rectum during Three-Dimensional Conformal Radiotherapy Treatment (3D-CRT) of prostate cancer compared to the baseline cancer risks in literature. The risk of induced-radiation cancer related with radiation treatment for patients with prostate cancer is of great importance in clinical radiation oncology. Therefore, the dose response relationship to predict radiation-induced secondary cancers was modeled for localised prostate cancer patients treated at Sweden Ghana Medical Centre (SGMC) over the past 5 years. Data of thirty patients' who received a total dose of 78 Gy with 39 fractions during treatment were selected. Dose-volume histograms from pelvic planning CT scans were used to determine organ equivalent doses (OEDs) for bladder and rectum using linear dose response, linear-plateau and competition models. From BEIR VII risk models, the age-dependent lifetime attributable risks to organs inside the primary beam with a known tendency for cancer was estimated using organ equivalent doses obtained. The estimated risks of radiation-induced cancer for bladder and rectum were in the ranges of 1.17 %-4.4 %, 0.14 % - 0.28 % and 3.4E-06 % - 1.6 %, and 0.38 % - 2.17 %, 0.19 % - 0.63 % and 2.05E-09 % - 0.11 % for linear dose response, linear plateau and competition models respectively. The risk estimations by these models were observed to be similar as compared to the range of risks available in literature except for the linear dose response model. Results confirm that patients who are younger, are at higher risk of developing secondary cancer later in their life time compared to older patients. The ideal models were found to be linear-plateau and competition model at high doses.

DEDICATION

I devote this thesis work to Lord God Almighty for His great love, wisdom, protection and care given me throughout my education. He deserves all the glory. My next dedication goes to my parents (Mr. Benjamin Osafo-Aye and Madam Sophia Yeboah) and my siblings for always being there for me.

ACKNOWLEDGEMENTS

I am full of praise for Elohim God for empowering me to reach such a point like this in my career, having granted on me mercies, grace and favour to complete this programme of study.

My deep gratitude goes to my supervisors Prof. Cyril Schandorf, Dr Stephen Inkoom and Mr. George Felix Acquah for their commitment, words of encouragement, corrections and guidance throughout my research and preparation for this thesis work. I say God richly bless you.

In a special way, l am particularly grateful to Mr. K.T Addison, my lecturer; Mr. Philip Oppong Junior of Sweden Ghana Medical Centre and the management of Sweden Ghana Medical Centre for allowing me to use their facility for my research work.

My heartfelt thank goes to my colleague Mr. Oswald Msosa Mkanda, for his help and support for this thesis work. It is a privilege knowing you, God bless you for your company throughout our studies.

TABLE OF CONTENTS

LIST OF TABLES

LIST OF FIGURES

LIST OF PLATES

LIST OF ABBREVIATIONS

3D	Three dimensional
3D-CRT	Three-dimensional conformal radiotherapy
B	Bladder
BEIR	Biological Effects on Ionising Radiations
BT	Brachytherapy
CC	Collapse cone
Com	Competition
CT	Computed Tomography
CTV	Clinical target volume
DICOM	Digital imaging and communications
DVH	Dose volume histogram
EBRT	External beam radiotherapy
GTV	Gross tumour volume
Gy	Gray
HDR	High dose rate
IAEA	International Atomic Energy Agency
IGRT	Image guided radiotherapy
IMAT	Intensity-modulated arc therapy
IMRT	Intensity-modulated radiotherapy
LAR	Lifetime attributable risk
LDR	Low dose rate
LE	Linear-exponential
LNT	Linear-no-threshold
LP	Linear-plateau
MC	Monte Carlo

MeV	Megaelecton-volts
MLC	Multi-leaf collimator
MPHIL	Master of Philosophy
MRI	Magnetic Resonance imaging
mSv	milli Sievert
MU	Monitor units
MV	Mega Voltage
NCRNM	National Center for Radiotherapy and Nuclear Medicine
NCRP	National Council on Radiation Protection and Measurements
NR	Not reported
NTCP	Normal tissue complication probability
OARs	Organs at risk
OED	Organ equivalent dose
OMP	Oncentra MasterPlan
PB	Pencil beam
PC	Computer
PET	Positron emission tomography
PTV	Planning target volume
R	Rectum
RIC	Radiation-induced cancer
SEER	Surveillance Epidemiological End Results
SGMC	Sweden Ghana Medical Centre
SRS	Stereotactic radiosurgery
TCP	Tumour control probability
TERMA	Total energy released in matter
TPS	Treatment planning system
UNSCEAR	United Nations Scientific Committee on the effects of

	Atomic Radiations
VMAT	Volumetric-modulated arc therapy

CHAPTER ONE

INTRODUCTION

1.0 Overview

This chapter presents the background, relevance and justification, statement of the problem, the scope and objectives of the research work and the structure of the thesis.

1.1 Background

Malignancy is a class of diseases portrayed by wild cell development which crowds out normal cells. The disease develops when mutated cells partition uncontrollably to form lumps and masses of tissue called cancers. Cancers can develop and meddle with body systems and discharge hormones that adjust body function. Tumours can either be benign (that is lumps that are not cancer) or malignant (that is lumps that are cancer). Tumours that exhibit restriction and stay in one spot development are by and large thought to be confined, while tumour that spreads to different parts of the body develops, attacking and annihilating other solid tissues or organs are said to have metastasized. Cancers are named according to the area or tissue of the body they have attacked, example cancer that attacks the prostate, breast is known as prostate and breast cancers respectively (Crosta, 2015).

Populace based growth registry in Ghana in 2012 (Laryea, et al.,2014) shows that the majority of tumours were recorded among females representing 69.6% of all cases. The average age of cancer incidences for all cases was 51.6 years. Among men, the mean age at findings was 48.4 years and 53.0 years for females. The commonest tumours

among men were cancers of the Liver (21.1%), Prostate (13.2%), Lung (5.3%) and Stomach (5.3%) (Laryea, et al., 2014).

Treatment of cancer involves several modalities which include chemotherapy (the utilisation of drug to execute disease cells or moderate their development), surgery (the removal of the tumour cell), radiotherapy (the use of ionising radiations to cure the disease or relieve pain), hormonal therapy and immunotherapy. Most often, these modalities are combined to make treatment strategy that is fitting for the patient and depends on patient tumour site and also persistent inclinations.

Radiotherapy is the utilisation of high-energy radiation (for example X-ray, gamma beams and charged particles) to shrink tumours and kill disease cells. Radiation treatment is performed either by a machine outside the patient body more usually by a linear accelerator or by cobalt-60 and is focused on the tumour site (external-beam radiation treatment), or radioactive materials put close or into the tumour cells (brachytherapy). This research is centred on external beam radiotherapy (EBRT).

In external beam radiotherapy (EBRT), a beam or many beams of gamma rays or high-energy X-ray are conveyed to a patient's tumour. These energetic x- ray beams can deposit their energy to the tumour area to destroy the malignancy cells and with careful treatment planning, spare the surrounding normal tissues. Three-dimensional conformal radiotherapy (3D-CRT) and Intensity Modulated Radiotherapy (IMRT) (Murray, et al., 2015) enhance the probability of tumour control and the likelihood of nearby normal tissue complications. (IAEA, 2008).

Unlike chemotherapy, a systematic treatment that spreads all through the body, radiation treatment is delivered precisely to one specific area, so harm to healthy tissues in the body is significantly less. Likewise, dissimilar to surgery, in which the infected

tissue is removed, radiation treatment is painless and non-invasive. In spite of the fact that radiation treatment can make less harm to the body and less extreme symptoms, it nevertheless presents the risk of both long and short term side effects. Among short term side, effects include skin rash, skin redness and skin sensitivity. Radiotherapy has always involved the avoidable irradiation of healthy organs and tissues outside the target volume. The detrimental effects of irradiation of critical organs are the probability of the induction of secondary cancer. A second malignancy is characterised as a histological discrete tumour that grows after first cancer (Bhatia & Sklar, 2002; Schneider, 2011). The development of malignancy because of radiation is a serious long-term side effect or risk of radiation therapy and is of great concern nowadays.

Second cancer risk outcome from the treatment of prostate cancers using 3D-CRT modality was estimated in this study, by the concept of organ equivalent dose (OED) and lifetime attributable risk (LAR) of radiation-induced cancers.

1.2 Statement of the Problem

In clinical radiation oncology, the risk of secondary malignancies related to radiation treatment for cancer patients is of incredible significance (John & Igor, 2015). The role of radiation treatment in patients treated with prostate tumour is continually increasing as a noninvasive treatment modality (Azvolinsky, 2012). Radiotherapy for prostate tumour has been connected with the risk of a late event of second cancers both in the pelvis and outside the targeted area because of radiation scatter from low doses Sountoulides et al., (2010); Azvolinsky, (2012). Secondary cancers after prostate irradiation incorporate dominantly rectum and bladder cancer. (Chrouser, et al., 2005; Baxer, et al., 2005; Boorjian, et al., 2007; Singh, et al., 2005; Brenner, et al. 2000; Azvolinsky, 2012).

However, determining this risk after radiotherapy presents a great challenge since secondary cancers have a dormancy period of onset of 5 or more years after the underlying treatment. In a bid to circumvent this challenge, several models have been proposed for assessing the risk of radiation-activated cancer from radiotherapy.

Sweden Ghana Medical Centre has been treating prostate cancers, among other types of cancer, using 3D-CRT and other techniques. There was the need to have a modeled dose response relationship to predict radiation-induced secondary cancers for localised prostate cancer patients who have had 3D-CRT treatment at the centre over the past 5 years and also to enhance the proficiency of treatment delivery going forward.

This work, therefore, seeks to estimate and assess the risk of radiation induced secondary cancer using linear no-threshold, linear-plateau and competition models.

1.3 Objectives

The principal objective of this study is to model second cancer risks for in-field and organs at beam border (bladder and rectum) in three-dimensional conformal radiotherapy of prostate carcinoma contrasted to the baseline cancer risks in literature.

The specific objectives of this work are:

- Estimate second cancer risk resulting from 3D-CRT technology for prostate cancer patients using organ equivalent dose (OED).
- Make appropriate recommendations from the findings.

1.4 Relevance and Justification

Improvement of cure rate with radiotherapy for prostate cancer has introduced new treatment modalities from 50 Gy to 78 Gy with the help of gold makers and image guided radiotherapy (IGRT). This is probably going to increase the rate of secondary

cancer; hence the need to have a dose response relationship of radiation induced second cancer resulting from treatment of prostate cancers with three-dimensional conformal radiotherapy (3D-CRT) procedures (Schneider, 2011).

1.5 Scope and Limitations

This work was carried out at Sweden Ghana Medical Center (SGMC). There are numerous issues and uncertainty in modeling the basic science for prostate cancer since the models are utilised for the relative comparison of various treatment designs with respect to tumour acceptance.

According to Schneider, "the long term risk from current radiation treatment methods have not yet been resolved and are possibly to become obvious for many years, due to the long expectancy time for strong tumour induction". (Newhauser & Durante, 2001; Schneider, 2011)

These study focussed on three main areas:.

The first is, evaluating the risk of a man developing prostate cancer in his lifetime.

Secondly, is the differential diagnosis and prognosis of aggressive versus nonaggressive cancer (Frame & Scant, 2015).

The third is developing new treatment method for advanced disease, additionally working out how best to utilise existing treatments for ideal impact.

1.6 Structure of the thesis

This thesis work covers five (5) chapters. Chapter one is an introduction to the research and provides an overview of the current state of knowledge relevant to the study. Chapter two is the reviews of existing literature relevant to the research problem. Chapter three focuses on the materials and methods used to conduct the study. The results obtained are presented and discussed in chapter four. Chapter five contains the conclusion of the study, recommendation and suggestion for further study.

CHAPTER TWO

LITERATURE REVIEW

2.0 Introduction

This chapter contains literature, articles and publications of materials relevant to this research study.

2.1. Techniques in Radiotherapy

There has been a considerable improvement in the field of radiotherapy. During the last decade, 3D-CRT and the execution of this system as conformal treatment has turned out to be promptly accessible in numerous facilities. Common for all present day radiotherapy systems is the utilisation of computed tomography (CT) to give a premise to PC based treatment techniques. This is in some cases joined by data from magnetic resonance imaging (MRI), or positron emission tomography (PET) to upgrade the nature of the division of target volumes and organs at risk (OARs) Brodin, 2010.

2.1.1 Three-Dimensional Conformal Radiotherapy (3D-CRT)

3D-CRT, often referred to as "conventional radiotherapy" is presently the most commonly used radiotherapy technique and it has been widely used over the last few decades. The principle consists of megavoltage radiation beams delivered by a linear accelerator from normally 2-5 different gantry angles with radiation fields shaped by a multi-leaf-collimator (MLC) to include the target volume and to reduce unnecessary irradiation of normal tissues (Brodin, 2010)

The wide use of powerful computers in radiotherapy has made a substantial impact on treatment planning and delivery. 3D-CRT treatment depends on 3D anatomic

information and utilises dose distributions that adjust to the shape of the prostate as closely as possible to the target volume (Sebestyen, 2011). This helps to avoid damaging the healthy tissue surrounding it, reducing the risk of side effects (Faiz, 2003).

The idea of "conformal dose distribution has likewise been extended to incorporate clinical objectives, for example, maximising tumour control probability (TCP) and minimising normal tissue control probability (NTCP). Accordingly, the 3D-CRT procedure envelops both the physical and biological methods of reasoning in accomplishing the desired clinical outcome" (Sebestyen, 2011). In spite of the fact that, 3D-CRT calls for ideal dose distribution, there are numerous obstacles to accomplishing these objectives. The significant confinement is the knowledge of the tumour extent. Depending on the invasive capacity of the disease, what is imaged is generally not the clinical target volume (CTV). It might be what is known as the gross tumour volume (GTV). Thus, if the CTVs drawn on the cross-sectional images do not fully incorporate the tiny spread of the disease, the 3D-CRT loses its importance of being conformal (Tanatar & Yakinci, 2007). "If any portion of the unhealthy tissue is missed or extremely under dosed; it will unavoidably result in failure despite all the care and effort expended in treatment planning, treatment delivery and quality assurance" (Faiz, 2003; Sebestyen, 2011). From the TCP perspective, exactness in restriction of CTV is more basic in 3D-CRT than in technique that utilisates liberally wide fields and less difficult beam plan to adjust for the instability in tumour localisation. "Patient motion, including that of tumour volume, critical organs and fiducial marks during imaging, simulation and treatment can give rise to systematic as well as random error that must be accounted when outlining the planning target volume (PTV)" (Sebestyen, 2011). If appropriate margins have been allowed for the localisation of PTV, the beam apertures conform and

effectively cover the PTV due its shape (example, “within 95% to 105% isodose surface comparative to prescribed dose”) (Faiz, 2003; Tanatar & Yakinci, 2007; Sebestyen, 2011). As a result of depth, radial distance, and tissue density, consideration must be given to the cross-beam profile, penumbra, and lateral radiation transport, in the plan of conformal fields to adequately treat the PTV. Sufficient margins must be given in between the PTV outline and the field boundary to ensure adequate dose to PTV at every treatment section. Regardless of the possibility; optimally designed fields, the biologic response for the tumour and the normal tissues needs to be considered in accomplishing the objectives of 3D-CRT (Faiz, 2003; Sebestyen, 2011). “In other words, the optimisation of the treatment plan has to be assessed not only in terms of dose distribution (example, dose volume histograms) but also in terms of dose-response characteristics of the given disease and irradiated normal tissues. Different models involving TCP and NTCP have been proposed, however, the clinical information to approve these models are rare. Until the reliable data are available, caution is needed in using these concepts to evaluate treatment plans. This is particularly vital in considering dose-escalation schemes that invariably test the limits of normal tissue tolerance within or in proximity to PTV” (Sebestyen, 2011). Various target volumes (GTV, CTV, PTV, etc.) should be carefully designed considering the inborn restrictions or uncertainties at each step of the procedure (Sebestyen, 2011). The last PTV ought to be constructed not just with respect to the “given imaging information and other diagnostic studies additionally the clinical experience that has been acquired in the management of that disease. Tightening of field margins around the imaged-based GTV, with the little consideration of occult disease, patient motion, or technical limitations of dose delivery, is a misuse of 3D-CRT concept that must be avoided at all cost” (Faiz, 2003; Sebestyen, 2011).

Conformal radiotherapy conforms or shapes the prescription dose volume to the planning target volume (PTV) as shown in figure 2.1 while in the meantime keeping the dose to specified organs at risk at doses underneath their tolerance dose. The conformal radiotherapy chain depends on 3D target localisation, 3D treatment planning, and 3D dose delivery techniques (Podgorsak, 2005).

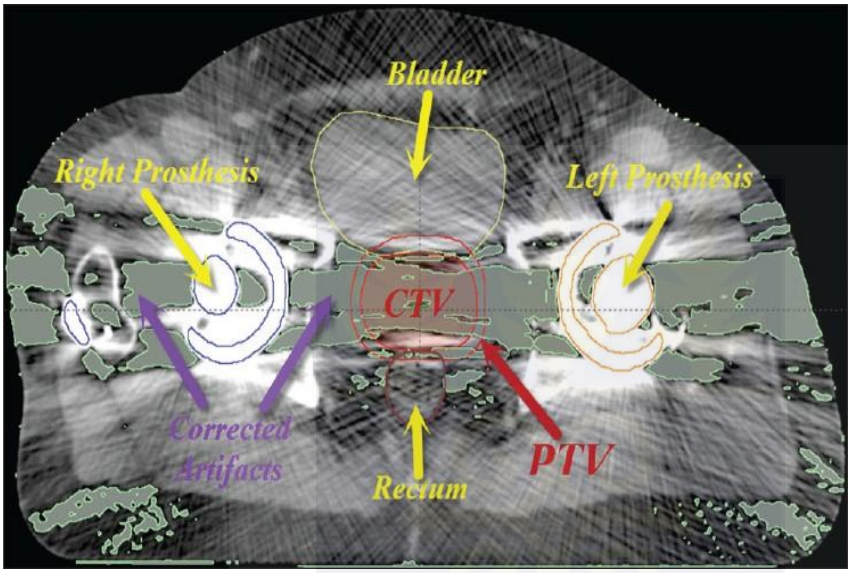

Plates 2. 1:3-D Conformal EBRT Target Volume Construction for Prostate Cancer

2.1.2 Intensity Modulated Radiation Therapy (IMRT)

Brahme, et al. (1982) was the first to propose IMRT in 1982. IMRT is an advanced kind of radiation treatment used to treat prostate cancer. With IMRT, the radiation beams are coordinated decisively with the size, shape and position of the prostate. The quality of the radiation beam can likewise be controlled with the goal that diverse regions get an alternate dosage all through treatment. This implies a higher dose of radiation can be given to the prostate, without making excessive harm to the surrounding normal tissue to constrain the side effects of treatment.

2.1.3 Image Guided Radiation Therapy (IGRT)

Imaging Guided Radiation (IGRT) is a type of cancer treatment that makes use of imaging technologies such as, Positron Emission Tomography (PET), Magnetic Resonance Imaging (MRI) and Computer Tomography (CT) during radiation treatment to improve accuracy and precision to deliver radiation to cancer cells. IGRT is utilised to treat tumours in territories of the body that move, for example, the lungs. Machines used in radiotherapy are equipped with imaging technology to allow the doctor to image the tumour before and during treatment. The patient is limited in the treatment room in an indistinguishable position as planned from the reference imaging taken during simulation (ACR, 2016). By comparing these images the radiation beam may be adjusted to more precisely target the radiation dose to the tumour. Some of these procedures use electromagnetic transponders or coloured ink tattoos, fiducial markers on the skin to align and target the radiation equipment (ACR, 2016).

2.2 Organ at Risk (OARs)

The organ at risk is an organ whose sensitivity to radiation is to such an extent that the dose gotten from the treatment plan might be huge compared with its tolerance, potentially requiring a change in the beam adjustment in the dose. Particular consideration ought to be paid to organs that, despite the fact that not immediately nearby the CTV, have a very low tolerance dose (example, the eye focal point amid nasopharyngeal or cerebrum tumour treatments). Organs with a radiation tolerance that rely upon the fractionation plan ought to be illustrated totally to prevent biasing during treatment plan assessment.

2.3 Modeling Secondary Cancer Risk

Radiation protection models are appropriate for evaluating radiation induced cancer (RIC) risk in low dose out-of field regions. A risk coefficient is applied to the equivalent dose the organ receives, which indicates the possibility of developing a secondary malignancy in a particular organ (Murray, et al., 2013). This risk coefficient is expressed in per cent per Sievert and consequently, the risk of second cancer increases in a linear fashion, as dose increases. The understanding that cells exposed to lower radiation doses are damaged, but not killed (or sterilised), by radiation, thus keep up the potential for malignant transformation is a linear function which depends on atomic bomb survivors Hall & Wuu, (2003); Murray, et al., (2013).

The relationship amongst dose and risk of second malignancy is less assured and several dose–response models have been proposed (Murray, et al., 2013) in high dose regions. These models take into account the harmony between induced radiation cell destruction, which leaves cells with the potential for malignant change, and cell sterilisation which renders cells unequipped for change Murray, et al., (2013). The linear-no-threshold (LNT) model, the linear-plateau (LP) model and the linear-exponential (LE) model are the most commonly utilised. Every one of the three shows a straight dose–response relationship for about the underlying 4 Gy of fractionated radiotherapy (Fontenot, et al., 2009; Hall & Wuu, 2003; Murray, et al., 2013). These three models demonstrate some variety at higher doses, the LNT model presumes an on-going linear relationship while LP model presumes a plateau in risk beyond the straight portion of the curve, and the LE model display recommends a diminishment in the risk (Murray, et al., 2013) because of increasing cell sterilisation at higher doses (Schneider, 2011; Murray, et al., 2013). It is contended that, as a general rule, these models speak to extremes, and it is possible that the genuine link lies somewhere close the LP and LE models (Hall & Wuu, 2003;

Murray, et al., 2013). The three models: LNT, LP, and LE do not take into account the impact of fractionation.

An additional model is the competitive risk model which likewise includes the impacts of effects of mutation induction at lower doses, and at higher doses cell killing. At lower doses, the relationship is nearly linear but then starts to decrease at higher doses, agreeing to a linear quadratic function (Dasu & Toma-Dasu, 2005; Murray, et al., 2013). This model likewise suits inhomogeneous dose distributions inside an organ and fractionation (Murray, et al., 2013).

2.3.1 The linear no-threshold (LNT) Model

The model suggests that cancer induced by radiation risk increases linearly with dose and is mostly based on data collected from atomic bomb survivors. This depends on exposures from 20-50 mSv up to several Sv and extrapolated down to zero doses. For exposures up to about 2.5 Sv this model is often referred to as the gold standard (Hall, 2006). The National Council on Radiation Protection and Measurements (NCRP) provided specific organ weighting factor can be used to estimate the cancer induction risk from exposure to different sites in the body yielding a total risk of 5%/Sv equivalent dose received (NCRP, 1993). This risk is assumed to be valid for the general population and an increase in risk to 15%/Sv has been proposed when regarding children (NCRP, 1993). For absorbed doses lower than 2 Gy this model is applicable for secondary cancer risk estimation but to organ, doses are often substantially higher when considering radiotherapy. In a study by Kry, et al., (2005), the secondary malignancy risk from different radiotherapy modalities was estimated using an LNT-model including equivalent doses up to 5 Sv (Hall, 2006).

2.3.2 The Organ-Equivalent Dose (OED) Model

This model was first introduced by Schneider et al. in 2005 as an attempt to provide a model of secondary cancer induction significant to patients undergoing radiotherapy (Schneider, et al., 2005). The basic rule of organ equivalent dose (OED) is that at low doses (< 2 Gy) the secondary cancer risk follows a linear relationship as in the LNT-model and the OED is the mean organ dose. At higher absorbed doses, as those mostly used in radiotherapy, Schneider et al. proposed that the OED follows a linear-exponential with the absorbed dose (bell shaped relationship). The idea of a bell shaped risk of cancer induction was first provided by Gray in 1957 proposing that cell killing effects overcome cell mutation at higher absorbed doses (Gray, 1965). The organ-specific OED for a bell shaped risk relationship is given by:

$$\text{OED}_{\text{org}} = \frac{1}{N}\sum_{i=1}^{N} D_i e^{-\alpha_{org} D_i} \qquad (2.1)$$

where N is the number of calculation points for each organ, D_i is the corresponding absorbed dose and α_{org} is an organ-specific parameter relating to the dose-response derived from fitting the model. The OED is defined such that a uniform irradiation of an organ to this dose will yield the same secondary cancer risk as the inhomogeneous dose-distribution on which the OED-calculated is based (Brodin, 2010).

The secondary cancer risk is by definition linearly dependent on the OED and can be calculated as using equation 2.2.

$$I^{org} = I_o^{org} \times OED_{org} \qquad (2.2)$$

where I^{org} is the organ-specific secondary cancer incidence relating to low-dose exposure (UNSCEAR, 2000).

The concept of OED has been applied to a plateau dose-response relationship as well, that is where the risk increases until a certain dose level after which it remains constant (Schneider, et al., 2005). Model parameters are established on Hodgkin's cohort as the original bell shaped model and OED for the plateau model is calculated using equation 2.3.

$$OED_{org} = \frac{1}{N}\sum_{i=1}^{N}\frac{1-e^{-\delta_{org}D_i}}{\delta_{org}} \qquad (2.3)$$

where δ_{org} is the organ-specific dose-response parameter gotten from fitting the model to the Hodgkin's cohort data (Brodin, 2010).

2.3.3 The competition risk model

As described by Dasu et al., (2005) the competing risks model is based on considering the probability of induced radiation cell mutation and the probability of cell killing as competing effects. With a dose- response relationship similar to the bell shaped one suggested by Gray, the competition model utilises a linear quadratic relationship to estimate cell mutation effects given in equation 2.4 (Dasu, et al., 2005).

$$Effect = (\alpha_1 D + \beta_1 D^2).e^{-(\alpha_2 D+\beta_1 D^2)} \qquad (2.4)$$

The first term of the product represents the cell mutation probability and the second term represents cell survival. Models described above are illustrated in Figure 2.1. for lung irradiation adopted from Brodin, (2010).

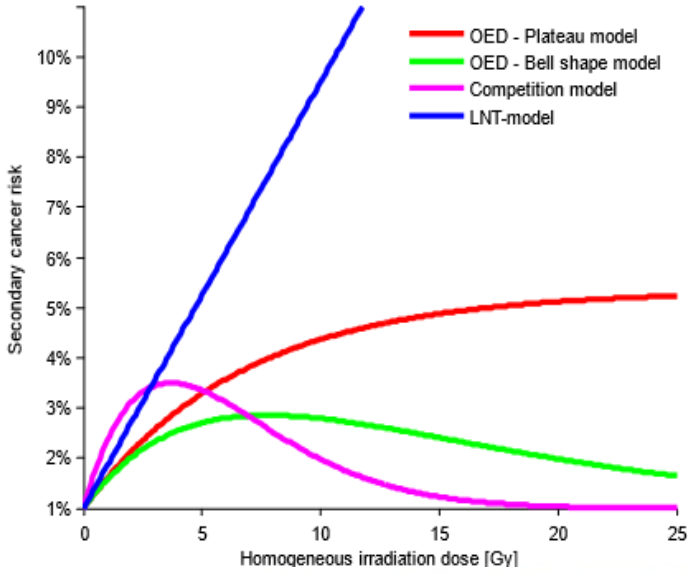

Figure 2. 1: Illustration of secondary cancer risk estimation due to lung irradiation providing a visual comparison between the different models for secondary cancer induction **(**Brodin**,** 2010**)**

2.4 Review Prostate Secondary Cancer

Most studies have concentrated on comparing the effect of different radiotherapy techniques on the likelihood of developing secondary cancers after radiotherapy.

2.4.1. Effect of IMRT vs. 3D-CRT

Relevant factors, when considering the effect of IMRT on radiation induced cancer (RIC) risk related to 3D-CRT, incorporate the outcome of an adjustment in distribution of dose and the escalation in monitor units (MU) necessary in conveying treatment (Murray, Henry, et al, 2013). These methods have two possible impacts (that is, dose distribution). In the first place, a bigger volume of normal tissue is irradiated to lower doses, which might contribute to increased RIC risk in in-field tissues and tissues in the immediate area (that is, tissues within the DVH volume, which is those included with the CT planning scan volume) (Hall & Wuu, 2003; Schneider 2011; Ruben, et al.,

2008 ; Murray, et al, 2013). The effects of this on RIC risk is influenced by the dose model utilised: theoretically, the LE model predicts increased RIC risk as a result of the low dose spread-out from IMRT, contrasted with the generally high doses and lack of low dose spread-out delivered with 3D-CRT (Murray, Henry, et al., 2013). As indicated by the LNT model, which predicts that RIC risk, will increase with dose, tissues receiving low dose spread-out from IMRT which would otherwise not have received such a dose with 3D-CRT, will naturally have a higher RIC risk. With a LP model, the impact of low dose spread-out will depend on whether that dose falls on the linear part of the curve (where risk increases with increasing dose) or the plateau part (where risk remains stable).

Secondly, however, the improved conformity of IMRT, and frequently accompanying smaller field sizes, may result in reduced scatter in nearby out-of-field tissues (for tissues between 15-30 cm from the field edge), thus reducing RIC risk (Ruben, et al., 2008; Lilliscrap, et al, 2000; Murray, et al., 2014). The IMRT conveyance involves increased MU, ensuing in increased machine leakage leading to increased out-of-field dose in tissues further from the field, which also increases RIC risk (Murray, et al., 2015; Murray, et al., 2013).

The comparative aid of the above mechanisms governs the extent of RIC risk. Within the PTV, the risk of (Murray, et al., 2014) RIC is known to remain fairly unchanged when moving from 3D-CRT to IMRT as there is little variation in the dose distribution within the target region itself, in terms of high doses (Hall & Wuu, 2003; Murray, et al., 2013). Table 2.1 presents a comparison between IMRT and 3D-CRT for risks of RIC (Murray, et al., 2013).

Table 2. 1: The risk of induced radiation cancers with IMRT compared to 3D-CRT

Authors	**Region examined**	**Method of acquiring information**	**Procedure of risk estimation**	**energy**	**% risk of second lethal harm**	
					3D-CRT	**IMRT**
Followill & Boyer, (1997)	Out of field	Phantom measurement	Whole body dose equivalent for photon NCRP risk coefficients	6 MV 18 MV 25 MV	0.6% 2.5% 4.5%	1% 4.5% 8.4%
Hall & Wuu, (2003)	In and out of field	Scanned volume (DVH). Scatter	LP LE	6 MV	1%	1.75%
Kry, et al., (2005)	Out of field	Phantom measurements	Organ specific dose equivalent for photon and neutrons NRCP risk coefficients	6 MV 10 MV 15MV 18 MV	NR NR NR 1.7%	2.9% 2.1% 3.4% 5.1%
Schneider, (2006)	In and out of field	Scanned volume (DVH). Photon scatter and neutron (phantom measurement)	Organ equivalent dose LE LP	6 MV 15 MV 18 MV	**15 MV 3D-CRT** 15% (LE) 1% (LP) 20% (LE) 2% (LP) 60% (LE) 30% (LP)	
Schneider, et al., (2007)	In and out of field	Scanned volume (DVH). Photon scatter and neutron (phantom	Organ equivalent dose LNT LE LP	15 MV **3D-CRT** 6 MV 15 MV	**100 Gy IMRT relative 70 Gy** 18.4%(LE) 15.0%(LP) 22.3%(LNT) 25.3%(LE) 17.0%(LP)	

		measurement			14.1%(LNT)
Ruben, et al., (2008)	In and out of field	Scanned volume (DVH). Photon scatter and neutron (phantom measurement	DVH analysis LE LP	18 MV 6 MV 6 MV	**3D-CRT** 1%(2.1%)(LP) 0.8%(1.5)(LE) **IMRT** 0.8%(1.7%)(LP) 0.6%(1.1%)(LE)
Bednarz, et al., (2010)	Out of field	Evaluated using MC simulations by computational phantom	BEIR VII coefficients	18 MV 6 MV	**3D-CRT** 0.03% stomach 0.3% colon 0.07% Oesophagus **IMRT** 0.04 % stomach 0.4% colon 0.07% Oesophagus

NR: not reported

Apart from the studies by Reuben et al., (2008) and Bednarz et al., (2010) the Table 2.1 suggests that IMRT results in increased RIC risk. The risk at which IMRT go on the rise as a result of increase in RIC risk at comparable energies is documented in other studies. This is generally ascribed to the increase in leakage as a result of increased MU requirements. Furthermore, the increased volume of normal tissues irradiated to a low dose is also a contributing factor (Hall & Wuu, 2003; Murray, et al., 2013).

Instead of comparing the impact within similar energies, the studies by (Bednarz, e tal., 2010) and (Ruben, et al., 2008), related higher energy (18 MV) conformal treatments with lower energy (6 MV) IMRT treatment, and found risks to be comparable (Murray, et al., 2013) as shown in the Table 2.1. Their evaluations are effective since in practice conformal plans will often employ higher energies while IMRT is often delivered using 6 MV.

It is recognised that at higher energies there is an increased contribution to out-of-field radiation from neutron production. The extent of this contribution and thus the absolute effect RIC risk is a matter of debate as a result of uncertainties regarding the radiation weighting factor which ought to be applied to neutrons and differences in the depths at which neutron doses are measured (Stathakis, et al., 2007; Stathakis, et al., 2009; Kry, et al., 2009; Murray, et al., 2013). The possible outcome of RIC danger due to photons that have high energies may give an idea about Bednarz, et al., (2010) and Ruben, et al., (2008) observation that there is insufficient difference in RIC risk.

Relating evaluated risk for RIC due to higher photon energy (15 or 18 MV) using three-dimensional conformal procedures with 6 MV, IMRT produces mixed outcomes with some studies and dose–response models (LP) assessing comparable levels of risk, some evaluation reduced risks and others estimated a persistently increased risk from 6 MV IMRT.

Table 2.1 presents evaluated comparative risk between 18 MV 3D-conformal radiotherapy and 6 MV IMRT which were obtained with LP and LE models.

2.4.2 Effect of Proton Therapy vs. IMRT and 3D-CRT

Studies assessing RIC risk after treatment with proton have reliably demonstrated a decreased risk relation with 3D-CRT and IMRT, irrespective of spot or passive

scanning methods utilised. Although, decrease in risk might be significant, Yoon et al. evaluated out-of-field RIC risk for protons to be about one-fifth lower than with IMRT. (Yoon, et al., 2010). The reduction in risk was largely due to reduced dose to non-target tissues as a result of the high conformity of proton treatments which results from reduced exit doses, and reduction in the volume of normal tissue irradiated. Close to the field, there is a reduction in secondary radiation with proton compared to photon treatments. At increased distances, the secondary doses from protons are higher, largely due to neutron production within the patient and machine head (Fontenot, Lee, & Newhauser, 2009)

The main special case to these perceptions was showed by Fontenot et al., 2010 when a weighting factor of 5 was applied to the neutron absorbed dose. With this weighting, RIC risk becomes comparable between proton and photon treatments. Bloch et al., (2010) likewise estimated uncertainties associated with risk evaluates. In terms of ratios of excess relative risk, there were only small uncertainties related to the dose–response model employed, while neutron weighting and inter-patient variability resulted in larger uncertainties (Fontenot, et al.,2010). Overall, uncertainties were in the order of +/−33%.

However, it should be noted that although RIC risk from protons is lower compared to IMRT using both spot and passive scanning techniques, passive scanning techniques result in much greater neutron production and so any reduction in RIC risk might be less with spot than passive scanning techniques (Murray, et al., 2013).

2.4.3 Impact of arc treatments

Alvarez, et al., (2009) examined RIC risk from quasi-IMAT (Intensity Modulated Arc Therapy), pseudo-rotational procedure employing equally spaced step of 36 and shoot beams to simulate an arc. Assessments were evaluated for quasi-IMAT and IMRT

utilising 36 and 72 segments. OED was utilised, using the LP and LE models, to relate the methods. Using LP and LE models, OED was similar. Murray et al., (2013) reported that a higher number of segments resulted in higher OED outside the scanned area (that is, out-of-field) for both IMRT and Quasi-IMAT. Most OED emanate from the primary beam (that is 88% and 86% for IMRT and quasi-IMAT respectively). Quasi-IMAT and IMRT resulted in similar OED with 36 segments. 72 segments were used at a point when, with quasi-IMAT there was a small increase in OED, however, this was not considered important. The escalation in relation to MU requirements resulted in increase (producing increased leakage) to deliver 72 segments quasi-IMAT. Despite normal irradiated tissues receiving low dose using quasi-IMAT due to the large number of beams, to sum up, RIC risk was significantly low for quasi-IMAT (Murray, et al., 2013).

2.4.4 Impact of Brachytherapy on Radiation induced Cancer

Takam et al., (2009) estimated the RIC risk following brachytherapy. Their study used the competitive risk model to evaluate risks from differential DVHs for the rectum and urethra. Estimates were evaluated for low dose rate (LDR) monotherapy (I-125), high dose rate (HDR) monotherapy (Ir-192), and combination 3D-CRT with HDR boost (Ir-192). The following results were obtained: for rectum and urethra, with low dose rate-brachytherapy (LDR-BT), estimated risks were $2.0x10^{-4}$ % ± $3x10^{-4}$ and $1.3x10^{-8}$% ± $7x10^{-8}$ respectively. For HDR monotherapy were $1.0x10^{-4}$ % ±$1x10^{-4}$ and $2.3x10^{-8}$% ±$7x10^{-8}$. Rectal cancer risk was estimated at 0.06% for external beam radiotherapy-brachytherapy (EBRT-BT). The study concludes that lowest RIC risks were in relation to HDR or LDR-BT monotherapy and were attributed to the cell kill at high equivalent doses received by small regions of nearby organs (Takam, et al., 2009).

Unfortunately, the group were unable to also evaluate the risk of bladder RIC as the ultrasound planning system did not include the whole bladder volume.

2.5 Second cancers risk factors

There are numerous known second cancers risk factors after radiotherapy ranging from patient related risk factors for the induction of secondary malignancies. Young people (below 50) diagnosed with primary cancer are related to an increased risk of second cancer. The reason for this age effects can be associated with either increased vulnerability of the underlying organ to the mutagenic effect of therapy at a younger age, the higher rate of cell proliferation during the early stages of development; genetic vulnerability or a longer period of follow up of the childhood cancer survivor cohort, which allows second cancers with typically long latencies to develop (Dasu, et al., 2005; Schneider, 2011; SEER, 2015).

Studies have shown that certain chemotherapeutic agents, mostly alkylating agents and topoisomerase II inhibitors, increase the risk of developing secondary cancer. In some cases, specific genetic changes caused by these agents explain the increased risk of leukaemia (Schneider, 2011; Bhatia & Sklar, 2002)

Second cancers risk factors under search include hereditary, cancer syndromes, gene-environment interactions, lifestyle choices and other medical difficulties associated with primary cancer treatment. Radiation treatment increases the risk of numerous second cancers in a dose-dependent manner. Most second cancers associated with radiotherapy occur in or near the area that was irradiated and most have a long latency (Bhatia & Sklar, 2002; Schneider, 2011)

CHAPTER THREE

MATERIALS AND METHODS

3.0 Introduction

This chapter focuses on the experimental framework for the study, the analysis of data, the calculation of organ equivalent dose and the estimation of radiation induced cancer risk due to selected prostate cancer treatment at Sweden Ghana Medical Centre.

3.1 Materials

The materials used for this study include:

- Oncentra MasterPlan treatment planning system (Nucletron, Oncentra MasterPlan TPS, version 4.3)
- Elekta Synergy PlatForm teletherapy unit (Elektra, Synergy 11 Platform, S/N 2486)

3.1.1 Oncentra MasterPlan Treatment Planning System

The treatment planning system (TPS) used at SGMC is Oncentra MasterPlan (OMP). The TPS has two dose calculation algorithms: Pencil Beam (PB) and Collapsed Cone (CC) algorithms. These algorithms are both model based on energy fluence and also include head scatter modeling.

The first model is based on a two dimensional PB convolution for volume integration. Inhomogeneities are handled by an equivalent path length correction for the primary dose contribution and a one-dimensional convolution along fan lines with an exponential for scattered radiation (Knoos, et al., 2006).

The second model is a CC convolution approach in which a ray-trace method through the irradiated object is utilised to get the total energy released in matter (TERMA) at all

points in the dose calculation matrix. The TERMA is separated into a primary part (collision kerma) and a scatter part, each of which is transported separately along 106 lines from the interaction point (Knoos, et al., 2006). The energy from each voxel intersected by a fan line in the irradiated medium is collected and deposited according to the elemental composition of the medium and density variations along the fan line.

The OMP is designed for digital imaging and communications (DICOM) integration, network and flexibility. OMP allows numerous sets of data points to be classified as applicator points. For OMP photon dose calculation, parameters such as energy deposition kernels, electron contamination kernels, fluence matrix, source size, head scatter, ionisation chamber perturbation are required.

3.1.2 Elekta Synergy PlatForm Teletherapy Unit

Sweden Ghana Medical Centre (SGMC) uses Elekta Synergy 11 platform linear Accelerator (LINAC) with a standard 80 MLC head shown in figure 3.1. The machine was installed in 2011. The equipment has both photon and electron energies. The photon energies produced are 6 MV and 15 MV while electron energies produced by the machine consist of 6 MeV, 10 MeV and 15 MeV. The machine has a specialised multi-leaf collimator 2 x 40 leafs and 1 cm leaf width at isocenter. A 30 cm x 40 cm wedge installed in the system permits a 40 cm maximum field size at isocenter. It is fitted with a motorised 60-degree wedge and an iBeam evo carbon fibre couch top. The treatment beams are collimated, filtered and monitored with the treatment head of the LINAC in order to produce a clinically useful radiation beam which delivers a uniform dose distribution at a specified depth in water, with the help of the MLC. The Medical Physicist calibrates the LINAC to deliver a specific radiation dose at the isocenter with a high degree of accuracy. The machine output is measured in monitor units (MU) in which individual machines are calibrated to deliver a specific absorbed dose per MU

(usually 1Gy/MU). In treatment delivery, this equipment is capable of three-dimensional radiotherapy (3D), intensity modulated radiotherapy (IMRT), volumetric-modulated arc therapy (VMAT) and stereotactic radiosurgery (SRS).

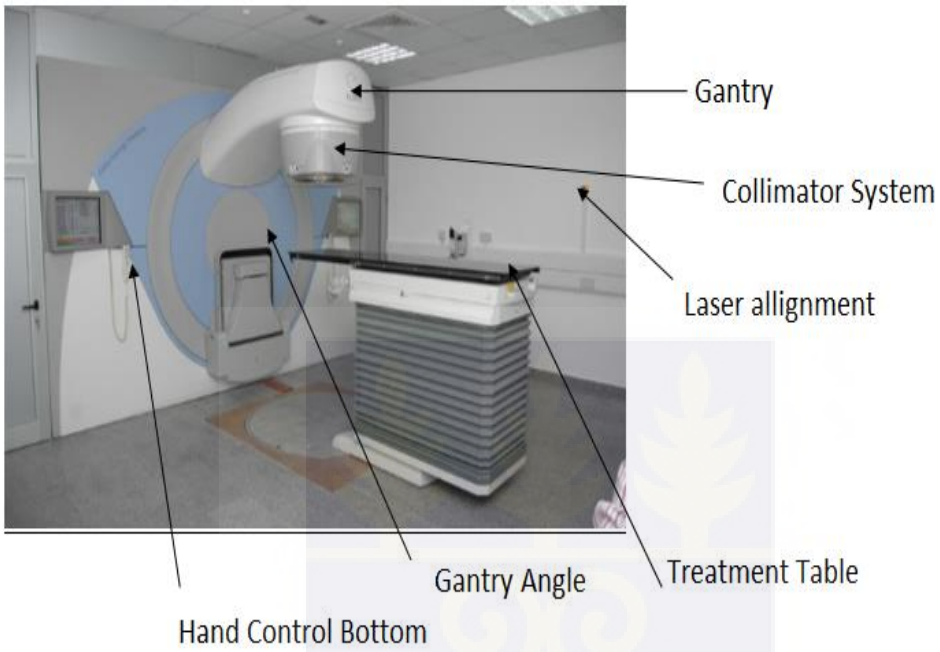

Plates 3. 1: Elekta Synergy Platform Teletherapy Unit

3.2 Experimental Method

3.2.1 Treatment Planning Protocol at Centre (SGMC)

- Insertion of three gold markers
- Full bladder and empty rectum scanning protocol
- CT/ MRI fused images
- 5 field beam arrangement planning
- Daily online image protocol

3.2.2 Patient Data

Thirty (30) male patients were selected with clinically diagnosed localised prostate cancers aged 50-79 years for this study. They had all received radiation therapy treatment for prostate cancer at Sweden Ghana Medical Centre. These patients were treated with three-dimensional conformal radiotherapy using 15 MV photon beam.

Each prostate cancer patient was instructed to drink 300 ml of water 30 minutes before treatment to fill the bladder and three gold markers inserted into the prostate for identification during treatment in case there is movement of the prostate

All treatment plans were generated using the OMP version 4.3 dose planning software and were based on computed tomography (CT) and magnetic resonance imaging (MRI) scans of the patients. Detailed patient data on absorbed dose received by bladder and rectum is presented in Table A.1 in the Appendix.

3.2.3 Target and OAR Delineation

The prostate, bladder, rectum and seminal vesicles were delineated by the Radiation Oncologist specialist. Clinical target volume (CTV) was defined as the whole prostate with involved seminal vesicles. The planning target volume (PTV) was designed using a uniform expansion around the CTV. Planning volumes for PTV were delineated with margins to the CTV during treatment planning to allow for setup uncertainty.

3.2.4 Treatment Planning Process

Treatment plans were generated for each of the thirty prostate patients. The modern prescription regimen is conventionally 75-79 Gy for standard risk patients (no confirmed metastases) and 78-80 Gy for high-risk patients (confirmed metastases). With

a conventional fractionation scheme (39 fractions of 2 Gy daily), each patient received a total dose of 78 Gy, to the isocentre, located at the centre of the PTV.

The plans were created with the aim of achieving high conformity level with the target coverage while attempting to spare OARs. These plans were created with at least three beams (anterior and posterior beams, right lateral and left lateral beams, oblique beams e.t.c) and weighted to obtain the best target coverage. The OARs (bladder and rectum) were shielded by fitting multileaf collimators (MLCs) to cover them but only to the extent that it did not compromise target coverage.

The plan acceptance criterion for the prostate patients was that more than 95% of the prescribed dose was delivered to more than 95% of the PTV volume (D95%). The following bladder constraints were used: V75 < 25%, V70 < 35% and V65 < 50%. For the rectum, the constraints were as follows V75 < 15%, V70 < 20%, V65 < 25%, and V60 < 35%

The radiotherapy plan for each patient during treatment planning was replanned. In relation to dose response in organ at risk, the rectum and bladder were divided into four equal parts on the planning CT. Four points were created on the rectum and bladder respectively as shown in figure 3.2 and 3.2 representing dose calculation points. Table A.2 containing detailed dose calculation points for each prostate cancer patient.

3.2.4: Treatment plan diagrams for bladder and rectum

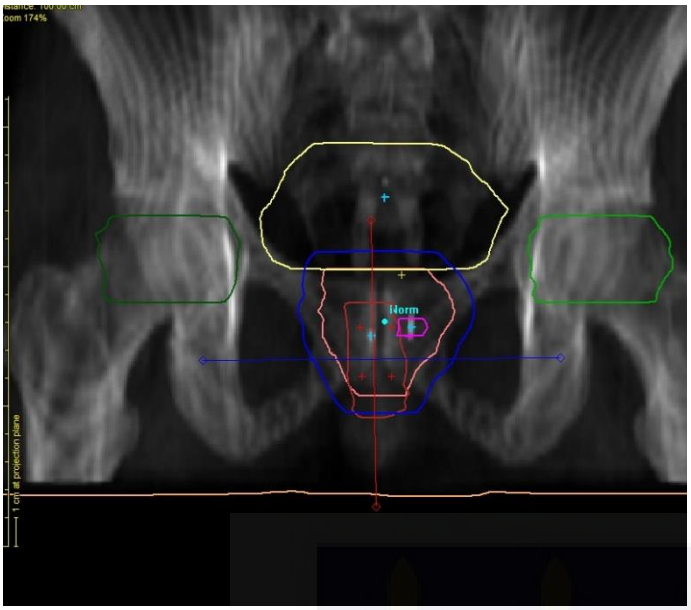

Figure 3. 1: Treatment plan for rectum

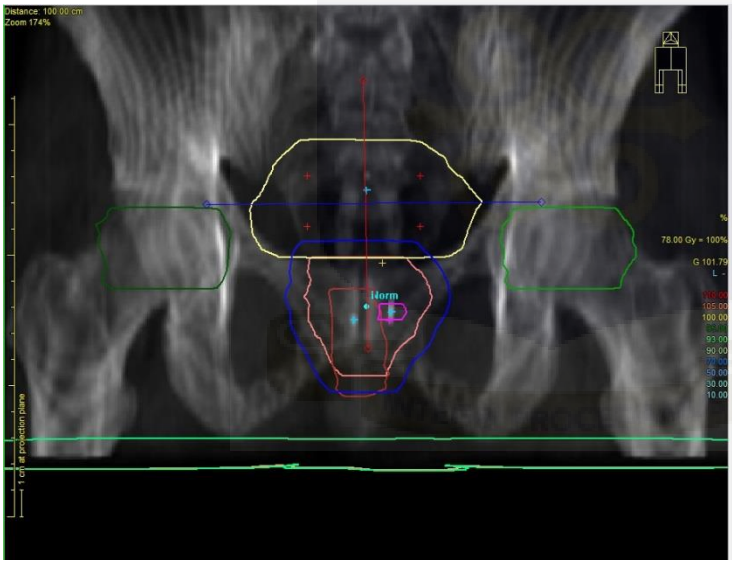

Figure 3. 2: Treatment plan for bladder

3.2.5. Second cancer risk estimation

Several models in relation to risk calculation for induced radiation second malignancy exist and the optimal is generally argued in literature. Schneider's concept of OED (this concept states that two different dose distributions which result in the same second

cancer risk have the same OED) which incorporates the effect of fractionation was adopted in this study (Schneider, et al., 2005). For higher doses where the dose response is not considered to be linear, the OED model was used to estimate the risk of rectal and bladder cancer by the:

a) Schneider's mechanistic model which includes specific repair/repopulation constant.
b) Competition model which suggest that the risk increases in a linear fashion with dose up to a threshold before decreasing due to cell kill at higher doses without tissue repair.
c) Plateau model which suggest that the risk increases initially in a linear fashion as dose increases up to a threshold at which risk levels off due cell sterilisation at higher doses with full normal tissue repair.

The dose-response relationships included in the subsequent analysis are described in the following with details about the model parameters listed in Table 3.1:

1. Linear dose –response (LNT):

$$\text{OED}_{\text{LNT}} = \frac{D_{mean}}{f_{red}} = \frac{1}{N f_{red}} \sum_{i=1}^{N} D_i \qquad (3.1)$$

where the DVH dose D_i is taken over N calculation points representing the relative organ volume. From Berrington et al., 2013 the linear risk reduction factor was applied at this stage.

2. Linear-plateau response (Schneider & Kaser-Hotz, 2005):

$$\text{OED}_{\text{Lin-Plat}} = \frac{1}{N} \sum_{I=1}^{N} \frac{1-e^{-\delta D_i}}{\delta} \qquad (3.2)$$

where δ is the organ-specific model parameter

3. Competition model, organ-specific bell-shaped dose-response for n fraction (Dasu, et al., 2011):

$$\text{OED}_{\text{Competition}} = \frac{1}{N}\sum_{i=1}^{N}\left(D_i + \frac{{D_i}^2}{(\alpha/\beta)}\right)e^{-\left(\alpha_2 D_i + \frac{\beta_2 {D_i}^2}{n}\right)} \qquad (3.3)$$

Where the cell survival parameters α_2 and β_2, α/β- value used were the original model parameters described in Dasu, et al., (2011).

It was assumed that age range 50-59= R (50) ,60-69=R (60), 70-79=R (70) etc.

According to Stokkevag, et al., (2015), gender, age and organ specific risk factors, R, corresponding to the low dose linear increase were subsequently applied in calculating the lifetime attributable risk (LAR):

LAR = OED × R (exposure age, gender, organ) (3.4)

Table 3. 1: Model parameters adopted from (Stokkevag, et al., 2015)

	Bladder	Rectum	Unit	Reference
α/β	7.5	5.4	Gy	(Dasu, et al., 2011)
α_2	2.50E-01	2.50E-01	Gy^{-1}	(Dasu, et al., 2011)
β_2	3.3E-02	4.6E-02	Gy^{-2}	(Dasu, et al., 2011)
δ	5.10	0.26*	Gy^{-1}	(Schneider & Kaser-Hotz, 2005)
f_{red}	19.78	5.04	-	(Berrington, et al., 2013)
R(50)	1.46E-02	1.65E-03	Gy^{-1}	(Berrington, et al., 2012)
R(60)	1.20E-02	1.20E-03	Gy^{-1}	(Berrington, et al., 2012)
R(70)	7.35E-03	6.00E-04	Gy^{-1}	(Berrington, et al., 2012)
R(80)	2.85E-03	1.50E-04	Gy^{-1}	(Berrington, et al., 2012)

* Colon parameter applied

CHAPTER FOUR

RESULTS AND DISCUSIONS

4.0 Introduction

This chapter outlines and discusses the results from the patient data collected, patient's organ equivalent doses (OEDs) and estimation of the lifetime attributable Risk (the absolute risk) of developing a radiation-related secondary cancer.

Linear-no-threshold model, linear- plateau model and the competition model were the three models used to estimate the secondary cancer risks.

4.1 Second Cancer Risk Evaluation using LNT model

The OED and the corresponding relative risk of second rectal and bladder cancer (LAR) for each of the patients undergoing 3D-CRT are shown in Figures 4.1 and 4.2. Table A.3 containing detailed estimates of the OED and LAR is presented in the Appendix.

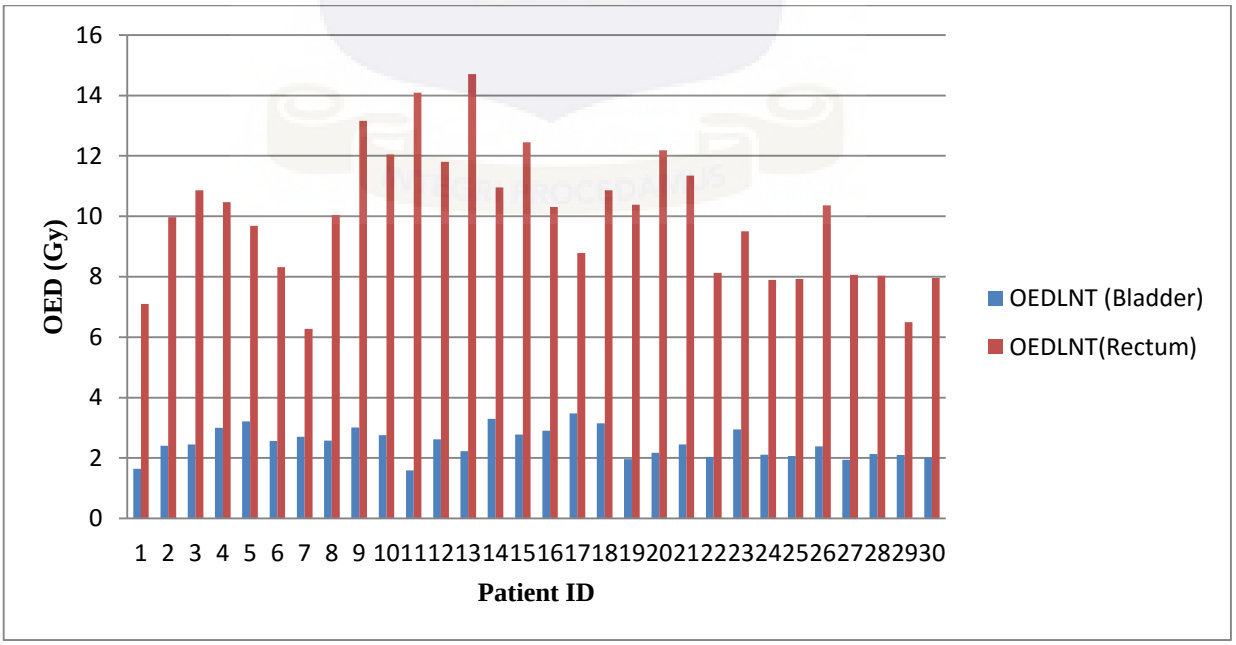

Figure 4. 1: Organ equivalent dose in bladder and rectum predicted using LNT

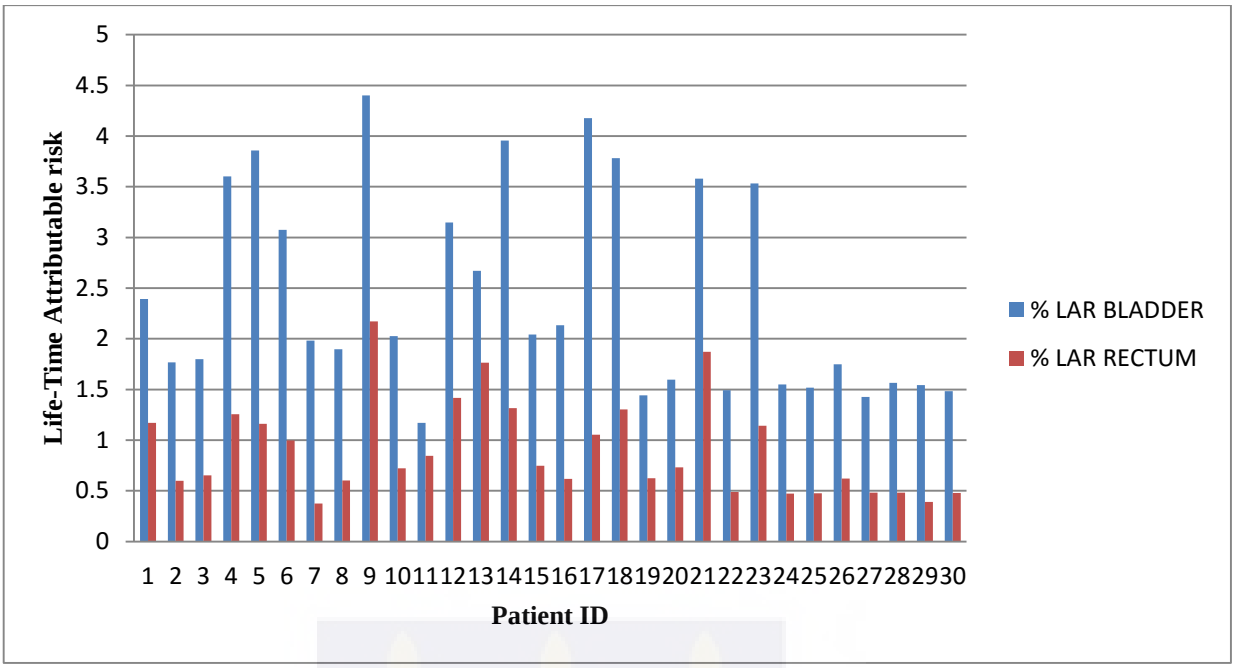

Figure 4. 2: Relative risk estimates of secondary cancer in bladder and rectum predicted using LNT model

The OED is the dose an organ receives. Figures 4.1, shows that OEDs to the bladder was lower than that to the rectum. Figure 4.2 shows the resultant increased radiation-induced second cancer risk for the bladder and is in the range 1.17 % and 4.4 %. Similarly, significant level of radiation induced cancer risk was observed in the rectum in the range 0.38 %-2.17 %. Low OED therefore implies that there is more mutation of the cell than cell killing, resulting in high risk of cancer recurring.

The graph is LAR versus patient ID and is dose dependent. For the LNT model, increasing the dose signifies increased risk. This proportional fit was observed in this study in which increase in dose resulted in a fairly linear increase in risk in both organs as shown in figure 4.3. Figure 4.3 also shows that the bladder was approximately three (3) times high risk of developing secondary cancer than the rectum. This could be due to treatment orientation or beam arrangement during planning or setup margin around the

PTV in order to achieve good target coverage. Detailed estimates for LAR using LNT model is presented in Table A.6 in the Appendix.

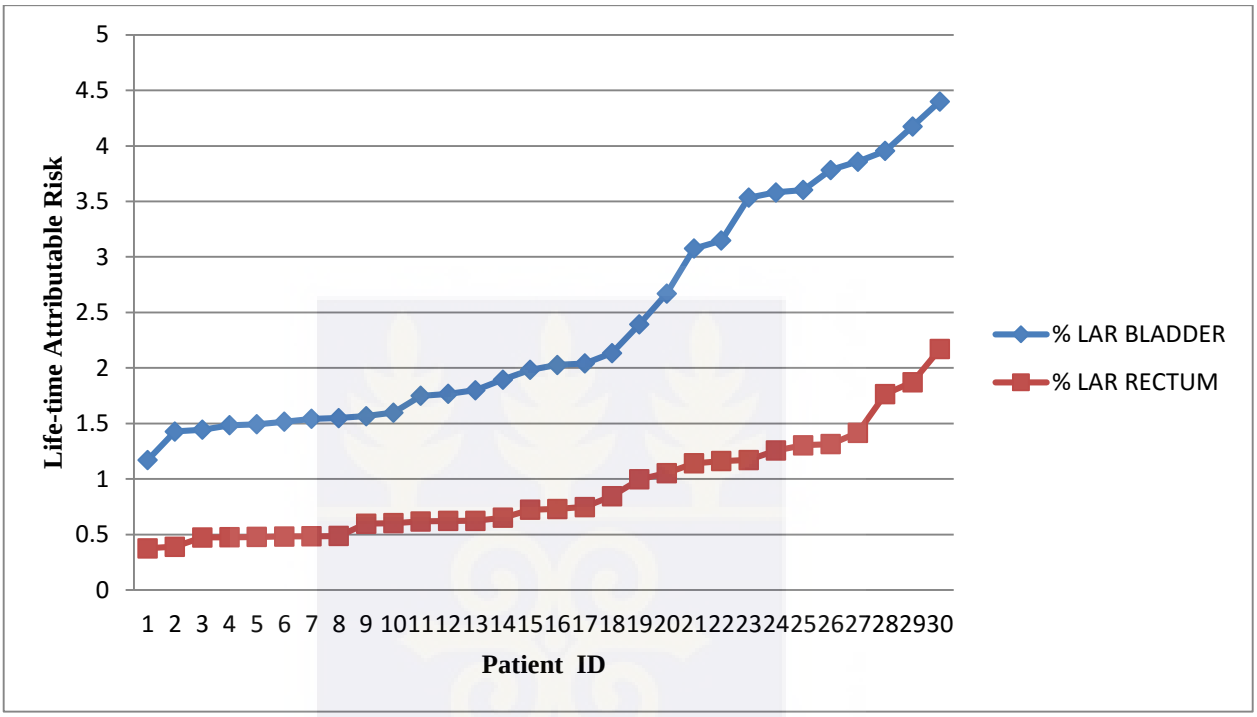

Figure 4. 3: LAR estimates for bladder and rectum using LNT model

Figure 4.4 shows results obtained when age was considered as a variable. Table A.7 containing detailed estimates of different age groups using LNT model presented in the Appendix. It was observed that there is an increased risk of developing secondary cancer for young patients, resulting in 2-3 % times higher risk of bladder and rectal cancer when patients were exposed to 50 years versus 70 years old because age is a fundamental risk factor for induced radiation second cancer.

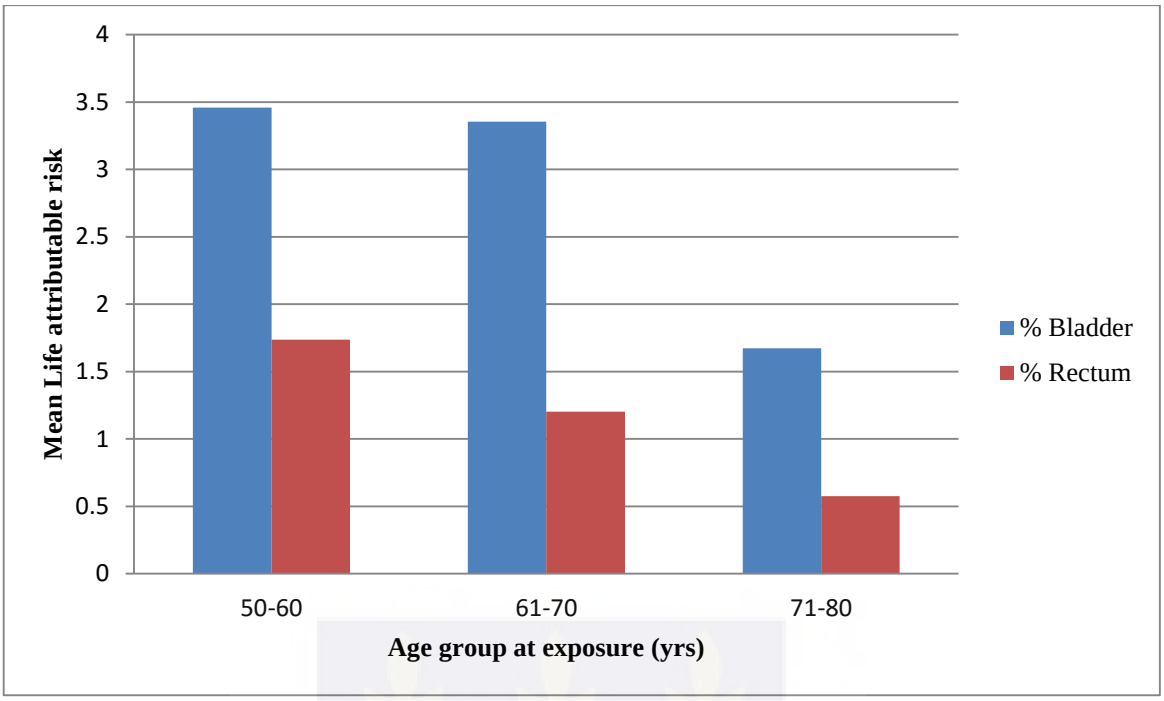

Figure 4. 4: Risk of radiation-induced secondary bladder and rectum cancer for age group based on exposure for LNT model

Several studies have reported similar results, Stokkevag et al., (2015) reported that even though the risks of radiation-induced bladder and rectal cancers were significantly small, the bladder demonstrated 2.1 times higher risk than the rectum. A significant increase of rectal cancer was found by Baxter et al. reporting incidences in the range 0.1-0.2 %. However most reported clinical results using LNT model indicate that the risk of secondary bladder cancer exceeds the risk of rectal cancer (Baxer, et al., 2005).

4.2 Second Cancer Risk Estimation using Linear Plateau model

Figures 4.5 - 4.6 shows the OEDs and LAR obtained when patient's data was evaluated using Linear-plateau model. Table A.4 containing detailed estimates of the OED and LAR is presented in the Appendix. From Figure 4.5, the rectum received high OEDs with little variation between individual patients as compared to the bladder, the corresponding risk estimate in the range of 0.29 % to 0.66 %. The lower bladder OEDs

resulted in lower risk estimates which were approximately 2 times lower than that of the rectum.

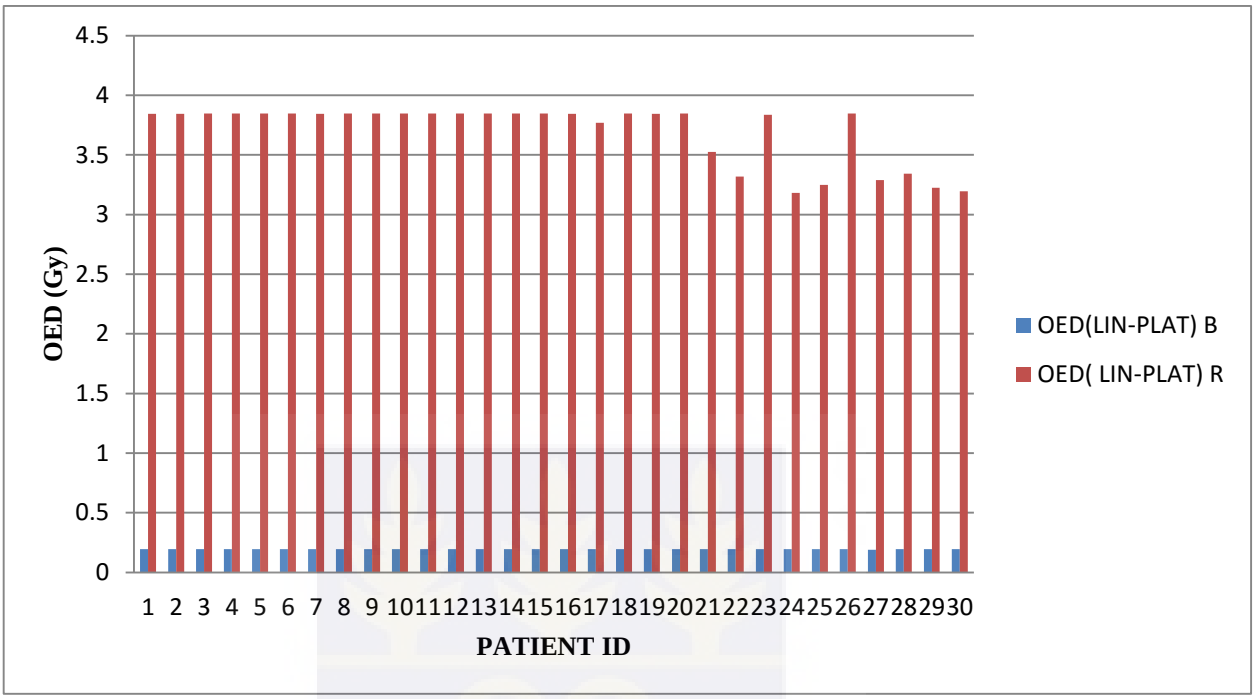

Figure 4. 5: Organ equivalent dose for bladder and rectum using linear plateau model

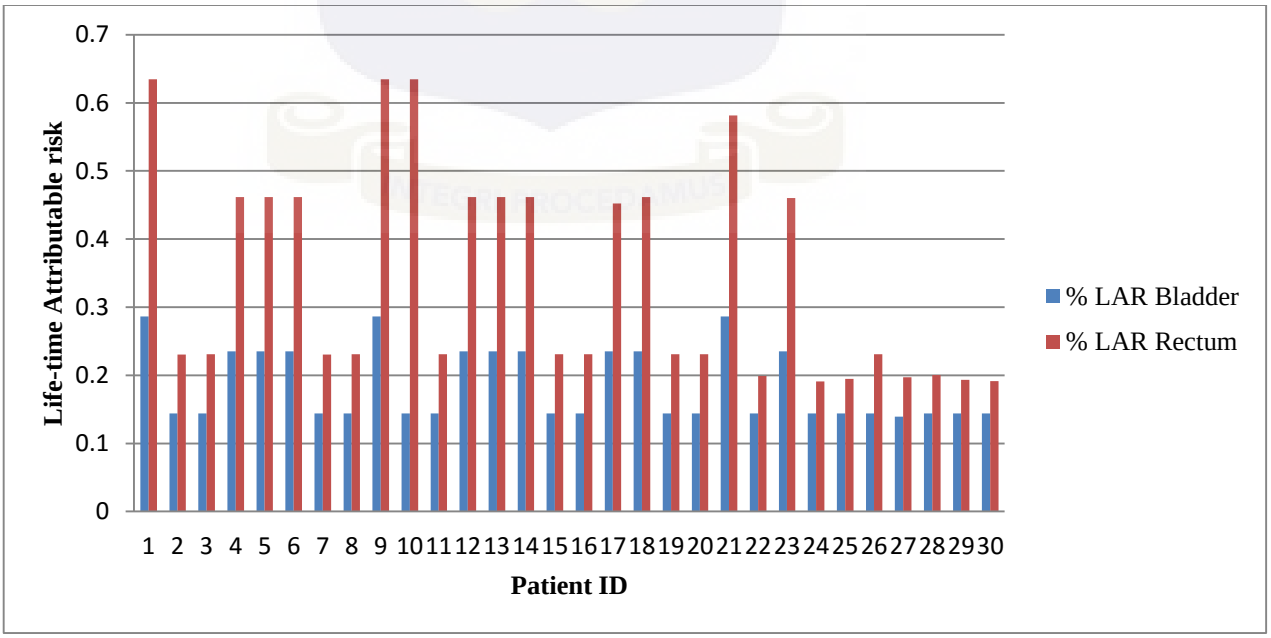

Figure 4. 6: Life Attributable Risk estimates for bladder and rectum when linear-plateau model was considered

The plateau model suggests that risk increases initially in a linear fashion as dose increases up to a threshold at which the risk levels off due to cell sterilization at higher doses with full normal tissue repair (Schneider, et al., 2011; Murray, et al., 2015) Figure 4.7 illustrates this phenomenon. Table A.8 containing detailed estimates of the OED and LAR is presented in the Appendix.

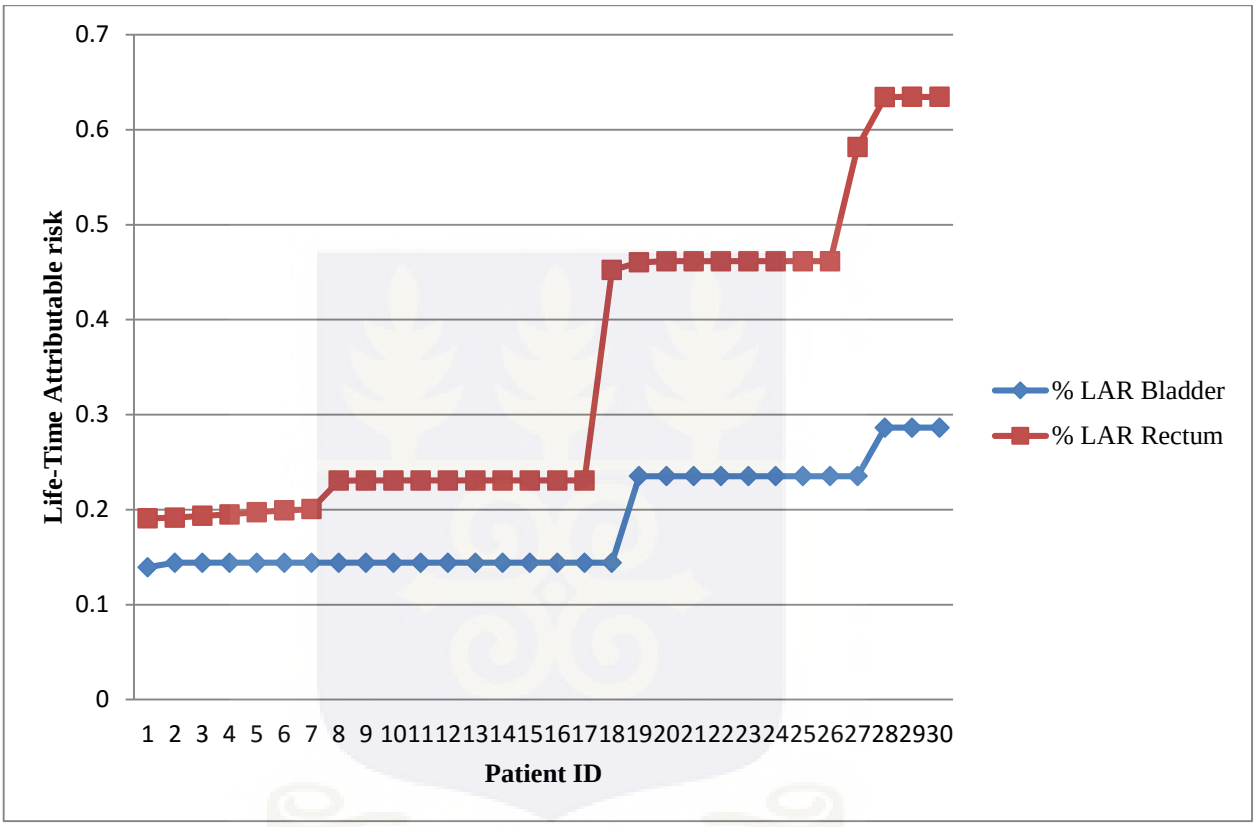

Figure 4. 7: LAR estimates for bladder and rectum for individual patients using linear-plateau model

There is epidemiological proof which proposes that after irradiation for cancer of the prostate most second malignancies emerge at areas which receive doses greater than 5 Gy, such as bladder rectum and bladder. The observation from this study agrees with Schneider's model (Murray, et al., 2015). Likewise, data obtained for irradiated cervical cancer patients suggests that there is an increasing dose–risk relationship for second rectal and bladder cancer for doses up to 60 Gy and greater. However, it has been

confirmed that the dose–risk relationship for second cancer for bladder and rectum bladder after irradiation for different primary tumour sites is essentially flat from doses of 1 to 60 Gy and other studies have also established that most second malignancy occurs at the edge of the PTV (Murray, et al., 2015; Epstein, et al., 1997; Dorr & Herrmann, 2002). One of these studies dealt with regions receiving a dose of 6 Gy or less.

Much the same as LNT model, the linear-plateau model showed that there was an increased risk of developing secondary cancer (6.4 %) for young patients (50-60 years) than older patients (71-80 years). Figure 4.8 shows the trend of LAR for different age groups in this study. Table A.9 containing detailed estimates of different age groups presented in the appendix.

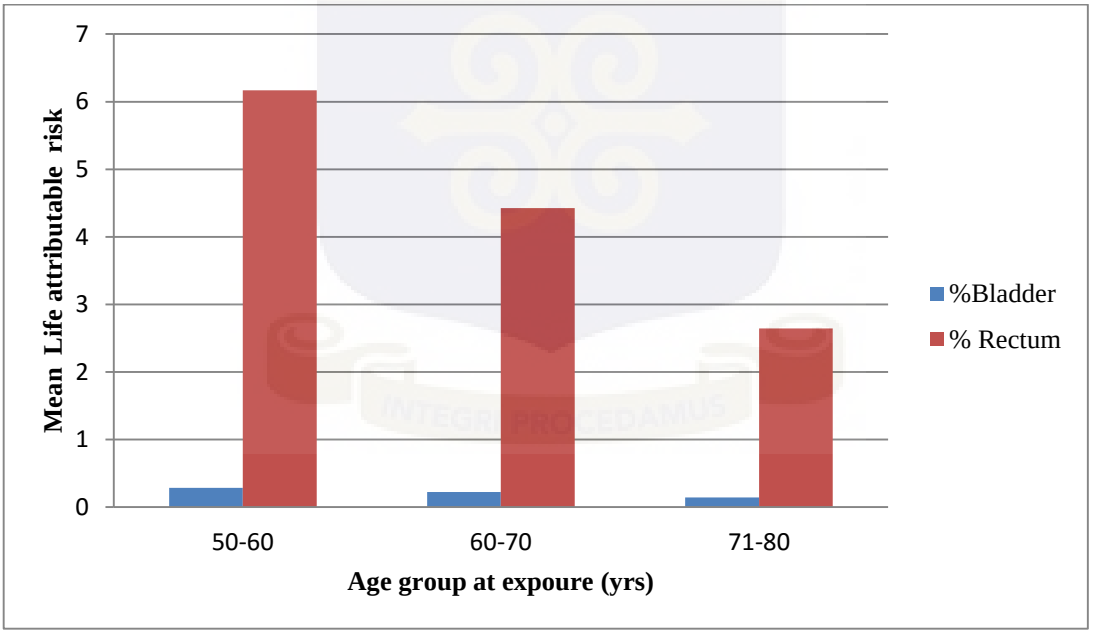

Figure 4. 8: Risk at exposure based on age group for linear-plateau model

4.3 Second Cancer Risk Estimation using competition model

Considering competition model, OEDs and risk estimation for each individual patient were calculated using excel. Figure 4.9 and 4.10 shows results obtained. Detailed estimates of OED and LAR using the competition model is presented in Table A.5 in the Appendix.

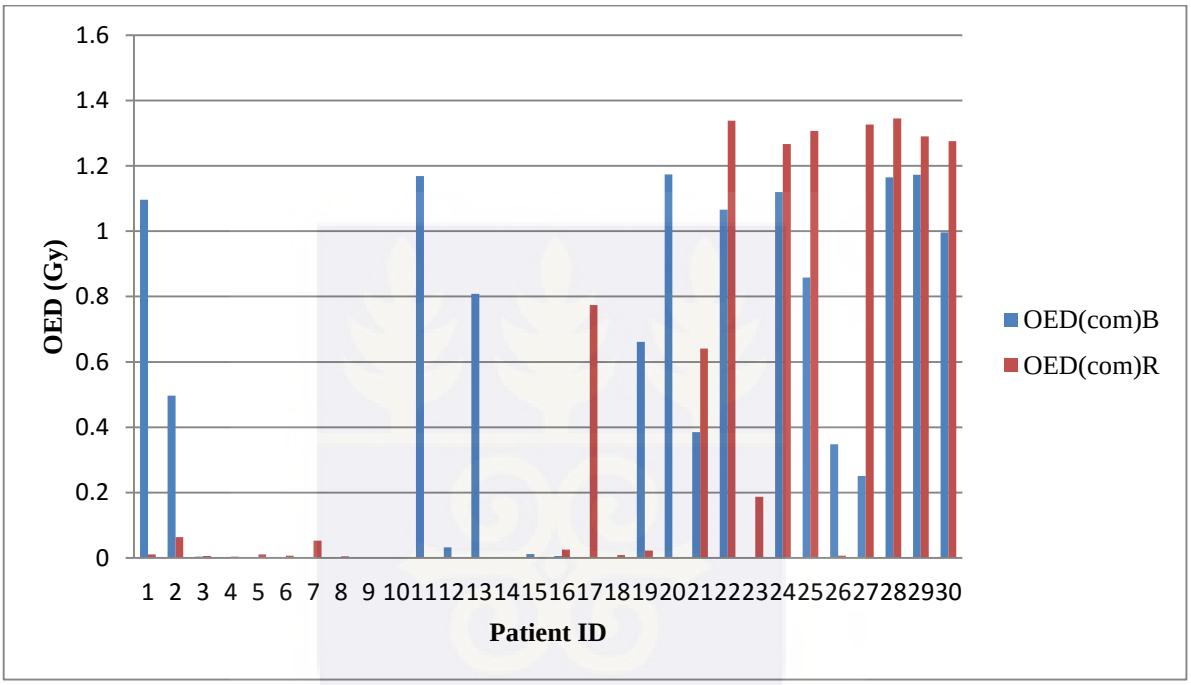

Figure 4. 9: OED in bladder and rectum for competition model

This shows that OEDs to the bladder was in the range 2.83E-06 Gy - 1.17 Gy as compared to that of the rectum in the range 1.71E -08 Gy – 1.35 Gy. Most of the patients received a low dose to the bladder and rectum, therefore, the probability of cancer induction is low for this model.

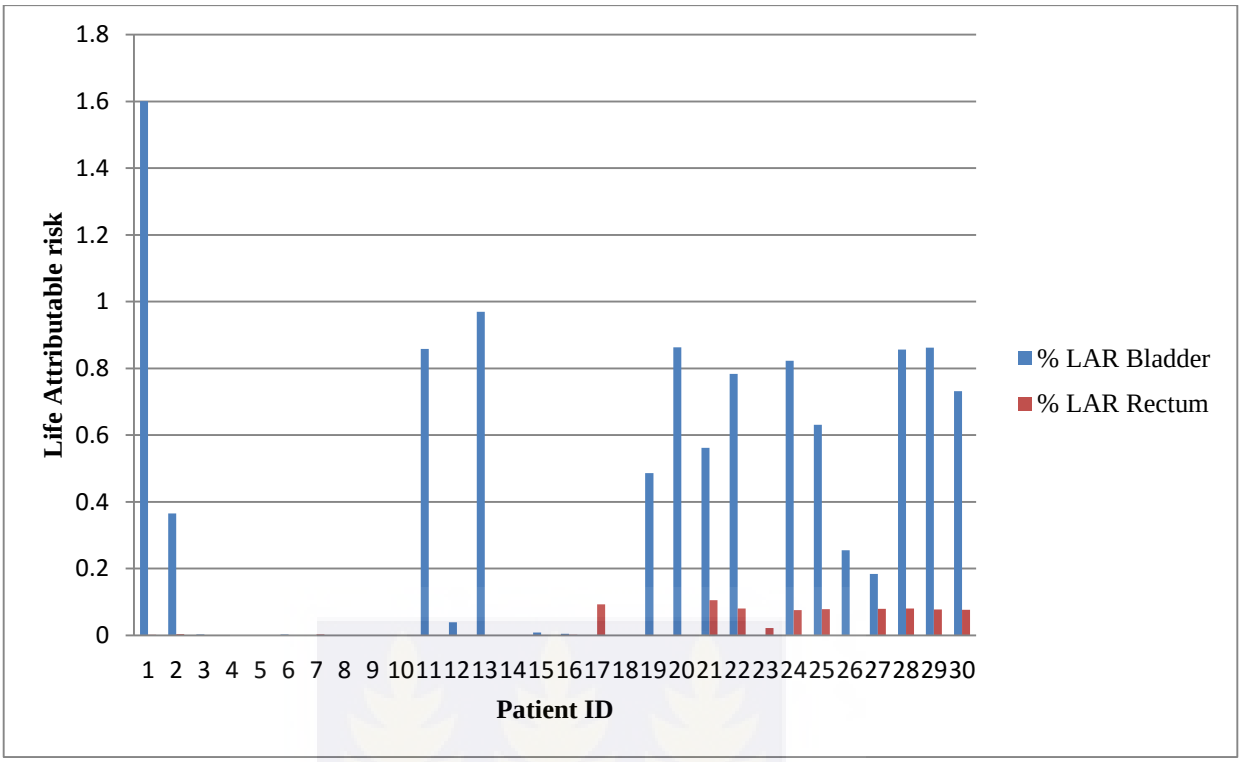

Figure 4. 10: LAR in bladder and rectum for competition model

An increase in risk estimate in the range 3.40×10^{-6} % - 1.60 % was observed in the bladder. Risk estimates for up to 43 % of the patients were very minute in both the bladder and the rectum. Risk estimates were generally below 2 % in the bladder for all patients

Figure 4.11 shows LAR relationship for each patient. Table A.10 containing detailed estimates of the OED and LAR is presented in the Appendix. As the dose increased, the risk of cancer induction also increased exponentially. However, the risk to the bladder was observed to be 16 times greater than the risk to the rectum.

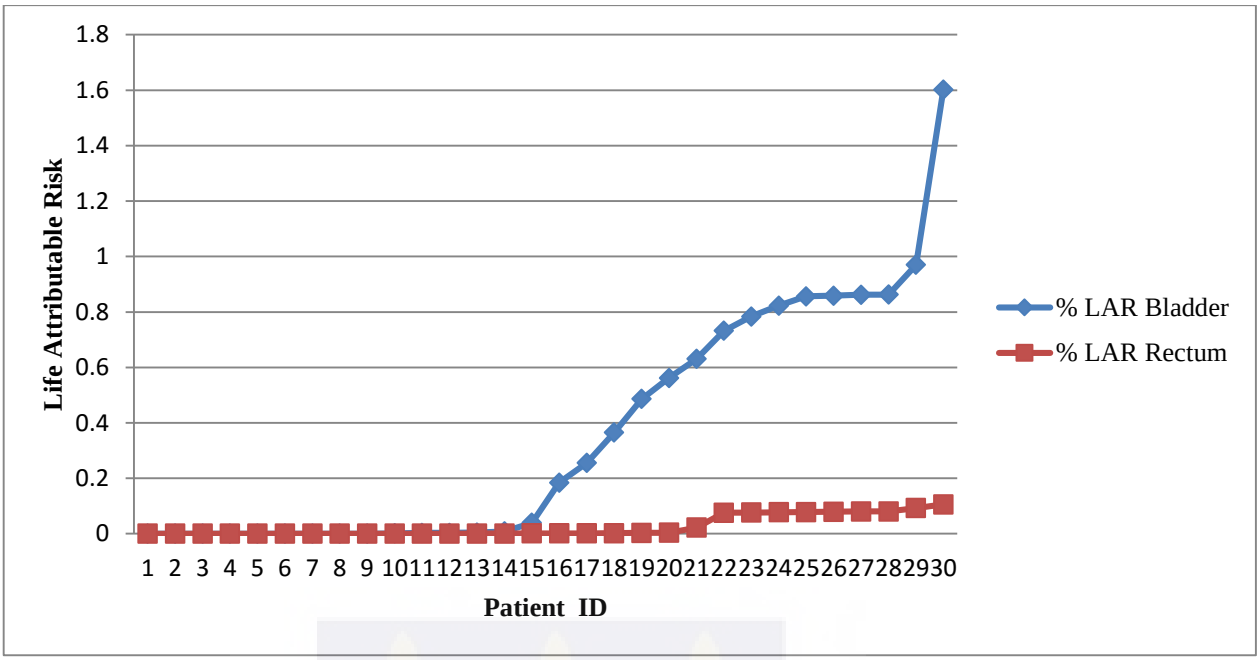

Figure 4. 11: LAR relationship for each patient using competition model

Figure 4.12 shows results obtained when age was considered in the range 50-60, 61-70 and 71-80. Table A.11 containing detailed estimates of different age groups using competition model is presented in the Appendix. For the age group 50-60, it was observed that there was an increased mean risk of developing secondary cancer resulting in 0.7 % of the risk in the bladder. 0.1 % and 0.4 % risk in the bladder for age group 61-70 and 71-80 respectively. There were little variations for patients in the age range 50-80 for rectum which implies low risk.

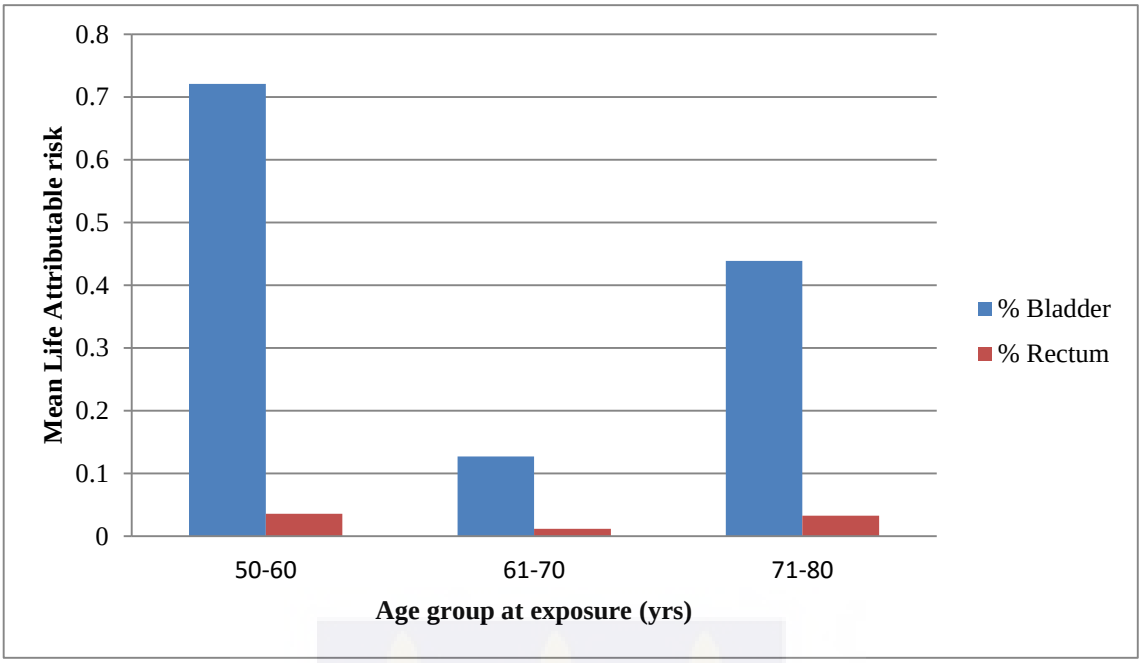

Figure 4. 12: Risk of induced cancer according to age at irradiation for competition model

4.4 Discussion

In this work, the risk of radiation-induced cancer for the bladder and rectum following 3D-CRT radiotherapy treatment of the prostate for 30 patients were assessed using three models proposed in literature.

It is generally agreed that the appearance of cancers following irradiation is a direct result of two competing processes; (1) induction of DNA mutation, leading to malignant transformations and (2) cell kill. While at low doses the total risk increases with increasing dose, at high doses cell survival decreases and the total risk of mutations significantly decreases as well (Upton, 1997)

From previously published data by Boice, et al., 1988 on prostate treatment, it can be inferred that, irrespective of the model and radiotherapy technique used, the risk for

radiation-induced secondary cancer in the bladder is about 0.15-0.32 % for an average dose above 30 Gy and that of the rectum is about 0.05-0.20 %. Though the average dose for the rectum is specified, it can be assumed that it is about the same order of magnitude as the dose to the bladder as two organs are irradiated at the same time during prostate treatment (Boice, et al., 1988)

Table 4. 1: Summary of risks estimated by the three models

Organ	**Bladder**			**Rectum**		
	Max (%)	**Mean (%)**	**Min (%)**	**Max (%)**	**Mean (%)**	**Min (%)**
LNT Model	4.4	2.4	1.17	2.17	0.90	0.38
Lin-Plat model	0.28	0.18	0.14	0.63	0.34	0.19
Competition model	1.6	0.36	3.40×10^{-6}	0.11	0.03	2.05×10^{-9}

Table 4.1 shows the summary of results of risks estimated for bladder and rectum in this study. According to the results, LNT model predicted the highest values of risks in both organs i.e. bladder =1.17 - 4.4% and rectum =0.38 -2.17%. These results are approximately 14 and 11 times higher than the clinically reported risks published by Boice, et al., 1988 for the bladder and rectum respectively. While studying the risk to the lung during the treatment of breast cancer, Inskip et al., (1994) established that induced radiation cancer risk for a mean dose of 10 Gy risk is around 0.9%. On the other hand, employing LNT model found a risk level of 17 % in the lung for an average dose of 10 Gy, i.e. one order of magnitude higher than the risk level observed by Inskip, et al., (1994). The group furthermore studied the irradiation of the bladder and rectum which result from a pelvic treatment of the prostate. In this case, the LNT model predicted maximum risks for secondary cancers of 19 % for the bladder and 78 % for

the rectum. Brenner et al., (2000) also found 37 % increase in bladder cancer and 12 % increase in rectal cancer.

The above-observed values seem completely unrealistic since such levels of incidence have not been encountered in practice. To a greater extent, these values demonstrate inherent limitation that may be introduced by the use of LNT model for radiotherapy application. One such limitation is that the use of linear model best works for low dose range such as atomic bomb survivors or therapeutic applications involving very low levels of irradiation from, for instance, low dose rate implants. In these scenarios, the irradiation of the organ is within the range where both linear and nonlinear models can predict almost the same result. However, in radiotherapy, in most situations, the doses received by the organ are so high that cell killing by radiation cannot be neglected.

The predictions obtained with Linear-Plateau and Competition models were observed not to be precisely at the intervals indicated by Dasu, et al., (2005) and Boice, et al., (1988). This is as a result of the differences in the used parameters that describe that the cellular survival and not necessarily the general principle of competition between induction and of mutation and cell kill. Despite this difference, intuitively the choice of parameters resulted in slightly modified predictions with less than one order of magnitude, but still considerably different from the LNT model. This observation was not surprising as the levels irradiations in radiotherapy results in significant cell killing.

Prostate irradiation often involves mean doses of the order of tens of Gy, which are well above the ‘window of opportunity’ (that is, dose level in which the risk of cancer induction is non-negligible). At this dose level, the cell killing is the dominant radiobiological response and therefore the number of cells with DNA mutation significantly reduced. This consequently leads to a negligible risk of cancer induction in

that organ. Hence the use of competition model in this study showed overall reduced risk for the bladder and the rectum than that in the case of LNT and Linear -plateau model.

The results observed in this study and in the aforementioned studies suggest that competition between induction of DNA mutations and cellular survival should be taken into account when estimating secondary cancer risk since the linear relationship model does not describe accurately the risk within the range of doses that may result from radiotherapy because of the nonlinearity of biological response to radiation.

Assuming age as a variable, all the models predicted a higher risk of radiation-induced cancer for a patient who received treatment at age 50 years than those at age 80 years. This observation concurs with one of largest studies on atomic bomb survivors, Life Span Study group. This group assessed that the relative risk of developing secondary cancer decreased by about 17 % per decade increase in age at exposure (John & Igor, 2015).

CHAPTER FIVE

CONCLUSION AND RECOMMENDATIONS

5.0. Introduction

This chapter provides the conclusions of this research work and recommendations from the findings to the stakeholders.

5.1. Conclusion

Three models for estimating cancer following radiotherapy treatment of the prostate cancer at Sweden Ghana Medical Center were explored in an attempt to investigate the importance of secondary cancer risks to the bladder and rectum in three-dimensional conformal radiotherapy (3D-CRT) compared to the baseline cancer risks in these organs as proposed in literature. Thus the results of this study were compared based on the interval proposed by Boice, et al., (1988).

In this work, results obtained confirmed that LNT model is not the appropriate model for estimating radiation induced cancer in dose ranges characteristic of radiotherapy. This is because in such dose ranges the competition between induction of DNA mutation and cell killing must be taken into account. Furthermore, the fractionation character of treatment and the non-uniformity of the dose distribution across the irradiated organ must be accounted for as these factors influence the estimation of the risks. Thus the estimations by this model were observed to be similar as compared to the range of risks proposed by Boice, et al., (1988).

Though the predictions obtained using the Linear-plateau and Competition models were observed not to be precisely within the proposed ranges, the results were in the same order of magnitude, indicating slightly higher or lower risks to both organs.

The results of this study also confirmed that younger patients are at the highest risk of developing secondary cancer later in their life time than those older patients.

5.2 Recommendations

5.2.1 Hospital Management

To the hospital, the following recommendations are made:

- Management should promote the culture of follow-up of prostate cancer patients treated after 5 years.
- Quality assurance and quality control should be done on regular basis to ensure that accurate delivery of dose to patients hence ensuring better treatment outcome and quality of life.
- Due to long term survival following treatment for younger prostate cancer patients with primary stage disease, the risk of radiation- induced second cancer should be taken into account when considering treatment options like brachytherapy (I-125).

5.2.3 Research Community

To the research community, the following recommendations are made:

- Further research can be extended, using male anthropomorphic phantom to verify scatter radiation dose during treatment for all the patients (using Gafchromic film or thermoluminescent dosimeters).
- Further study can be conducted to estimate risk for prostate cancer patients treated at Korle-Bu Radiotherapy Center and Komfo Anokye Radiotherapy Center in Kumasi.

- Further study can also be conducted to estimate risk for all cancer patients undergoing external beam and brachytherapy treatment.

LIST OF REFERENCES CITED IN MAIN TEXT

ACR, A. C. (2016, March 21). *Radiologyinfo.org for patients*. Retrieved from February 1, 2017 https//www.radiologyinfo.org

Alvarez, M. J., Koelbl, O., & Bogner , L. (2009). Quasi-IMAT technique and secondary cancer risk in prostate cancer. *Strahlenther Oncol*, 185(4):248-253. 10.1007/s00066-009-1931-x.

Arbea, L., Ramos, L., Martinez-Monge, Moreno, M., & Aristus, J. (2010). Intensity-modulated radiation therapy (IMRT) vrs 3D conformal radiotherapy (3DCRT) in locally advanced rectal cancer (LARC): dosimetric comparism and clinical implication. *Radiat Oncol*, 5:17. 10.1186/1748-717X-5-17.

Ayarous, A. (2014). Measurement and Comparism of Skin Dose Distribution in water Phantom exposed to 6 MV Photom beam . *Journal of Applied Sciences*, 14: 1952-1958.

Aziz, M. H., Schneider, A., Clausen, S., Blank, E., Herskind, C., Afzal, M., & Wenz, F. (2011). Can the risk of secondary cancer induction after breast conserving therapy using intraoperative radiotherapy (IORT) with low x-rays. *Radiat Oncol*, 6:174. 10.1186/1748-717X-6-174.

Azvolinsky, A. (2012). The walnut. *Newsletter of Prostate cancer canada network ottawa*, (613) 828-0762.

Baxer, N. N., Tepper, J. E., Durham, S. B., Rothenberger, D. A., & Virnig, B. A. (2005). Increased risk of rectal cancer after prostate radiation: A popoulation-Based Study. *Gastroenterology*, 128:819-824.

Bednarz, B., Athar, B., & Xu, X. (2010). A comparative study on the risk of secondary primary cancers in out-of-field organs associated with radiotherapy of localised prostate cacinoma using "Monte Carlo-based accelerator" and patient models. *Medical Physics*, 37(5):1987-1994. 10.1118/1.3367012.

Berrington, de Gonzalez A., E., Gilbert, Curtis, R., Inskip, P., Kleinerman, R., Morton, L., Rajaraman Preethatha, & Little, Mark P. (2013). Second solid cancers after radiation therapy: a systematic review of the epidermiological studies of the radiation dose-response relationship. *int J Radiat Oncol Biol Phys.*, 86:224-33.

Berrington, de Gonzalez A., Lulian , A., Veiga, L., Rajaraman, P., Thomas, B., Owen, H., Gilbert E, & Land C. (2012). RadRAT: a radiation risk assessment tool for lifetime cancer risk prrojection. *J Radiol Prot.*, 32:205-22.

Bhatia, S., & Sklar, C. (2002). Second cancers in survivors of childhood cancer. *Nat. Rev. Cancer 2*, 124-132.

Boice, J. D., Engholm, G., Kleinerman , R., Blettner, M., Lisco, H., Moloney, W., Donald F. Austin, Antonio Bosch, Diane L. Cookfair, Edward T. Krementz, Howard B. Latourette, Hans H. Storm, Elizabeth Bjorkholm, James A. Merrill, Lester J. Peters, Milford D. Schulz, C.M. Janine Bell, Michel P. Coleman, Patricia Fraser, Frank E. Neal, Patricia Prior, N. Won Choi, T. Gregery Hishop, Maria Koch, Nancy Kreiger, Dorothy Robbs, Diane Robson, D.H. Thompson, H. Lochmuller, Dietrich von Fournier, Rolf Frischkorn, Kjell E. Kjorstad, Arja Rimpela, Marie-Helene Pejovic, Vera Pompe Kirn, Hanna Stan Kusova, Franco Berrino, Kristjan Sigurdsson, George B. Hutchison & MacMahon Brain. (1988). Radiation dose and second cancer risk in patients treated for cancer of the cervix. *Radiat Res*, 116,3-55.

Boorjian, S., Cowan, J., & Konety, B. (2007). Bladder cancer incidence and risk factors in men with prostate cancer: results from Cancer of the Prostate Strategic Urologic Research Endeavor. *J Urol*, 177: 883-7; discussion 887-8.

Brahme, A., Roos, J., & Lax, I. (1982). Solution of an integral equation encountered in rotational therapy. *Phys Med. Biol Oct;27*, (10):1221-9.

Brenner, D., Curtis , R., Hall, E., & Ron, E. (2000). Second malignancies in prostate carcinoma patients after radiotherapy compared with surgery. *Cancer*, 88:398-406.

Brodin, P. (2010). Radiobiological optimization including consideration of secondary cancer risk: A treatment modality comparison study for paediatric meduloblastoma. *J Urol*, pp.9.

Chrouser, K. L., Bergstralh, E., Zincke, H., & Blute , M. (2005). Bladder cancer risk following primary and adjuvant external beam radiation for prostate cancer. *J Urol*, 174: 107 - 10; discussion 110-1.

Committee., B. V. (2006). Health Risks from Exposure to Low Level of Ionising Radiation. *The National Academics: Washington, DC, USA*.

Crosta, P. (2015, November 24). Retrieved 04 24, 2017, from Medical News Today: http://www.medicalnewstoday.com

Dasu, A., & Toma-Dasu, I. (2005). Dose-effect models for risk-relationship to cell survival parameters. *Acta Oncol*, 44(8):829-835. Epub 2005/12/08 10.1080/02841860500401159.

Dasu, A., Toma-Dasu, I., Franzen, L., Widmark, A., & Nilsson, P. (2011). Secondary malignancies from prostate cancer radiation treatment: a risk analysis of the influence of target margins and fractionation patterns. *Int. J Radiat Oncol Phys.*, 79:738-46.

Dasu, A., Toma-Dasu, I., Olofsson, J., & Karlsson, M. (2005). The use of risk estimation models for the induction of secondary cancers following radiotherapy. *Acta Oncol*, 44(4):339-47.

Dorr, W., & Herrmann, T. (2002). Cancer induction by radiotherapy: Dose dependence and spatial relationship to irradiated volume. *J. Radiat. Prot.*

Epstein, R., Hanham, I., & Dale, R. (1997). Radiotherapy-induced second cancers:are we doing enough to protect young patients? *Eur J Cancer*.

Faiz, K. M. (2003). *The Physics of Radiation Therapy, 3rd ed.* U.S.A: Philadelphia: Lippincott & Wilkins, pp. 465-474.

Followill, D., & Boyer, A. (1997). Examinates the whole-body dose equivalency produce by beam intensity conformity modulated therapy. *Radiat Oncol and Phys*, 38(3):6.

Fontenot, J., Bloch, C., Followill, D., Titt, U., & Newhauser, W. (2010). Estimates of uncertainties in the relative risk of secondary malignant neoplasms following proton therapy and intensity-modulated photon therapy. *Phys Med Biol*, 55(23):6987-6998. 10.1088/0031-9155/55/23/S02.

Fontenot, J., Lee, A., & Newhauser, W. (2009). Risk of second malignant neoplasms from proton therapy and intensity-modulated x-ray therapy for early stage prostate cancer. *Int J Radiat Oncol Biol Phys*, 74(2):616-622. 10.1016/j.ijrobp.2009.01.001.

Frame, L., & Scant. (2015, June 15). *Current challenges in prostate cancer: an interview with Prostate Cancer UK*. Retrieved January 20, 2017, from BMC Medicince: http://www.bmcmedicince.biomedcentral.com

Gray, L. (1965). In: Cellular radiation biology: A symposium considering radiation effects in the cell and possible implications for cancer therapy. *Baltimore: William & Wilkins*, 8-25.

Hall, E. (2006). Intensity-modulated radiation therapy, protons, and, the risk of second cancers. *Int J Radiat Oncol Biol Phys; 1 May*, 65(1) : 1-7.

Hall, E., & Wuu, C. (2003). Radiation-induced second cancers: the impact of 3D-CRT and IMRT. *Int J Radiat Oncol Biol Phys* , 56(1):83-88.

Hegamann, N.-S., Schlesinger-Raab, A., Ganswindt, U., Horl, C., E. Combs, S., Holzel, D., Jurgen E. Gschwend, Christian Stief, Claus Belka & Jutta Engel (2017). Risk of second cancer following radiatherapy for prostate cancer: a population-based analysis. *Radiat Oncol*, 12:2. 10.1186/s13014-016-0738.

IAEA, I. A. (2008). Transition from 2-D Radiotherapy to 3-D Conformal and Intensity Modulated Radiotherapy. *IAEA-TECDOC*, -1588, IAEA, Vienna.

ICRP. (2007). The 2007 Recommendations of the International Commission on Radiological Protection. . *ICRP Publication 103 Ann. ICRP, 37*, 1-332.

ICRU, I. C. (1985). *"Prescribing' recording andreporting photon beam therapy"*. U.S.A: ICRU Publication.

ICRU, I. C. (1999). *"Prescribing, recording and reporting photon beam therapy (Supplement to ICRU Report 50"*. Bethseda, Maryland, U.S.A: ICRU Publication.

Inskip, P., Stovall, M., & Flannery, J. (1994). Lung cancer risk and radiation dose among women treated for breast cancer. *J Natl Cancer Inst*, 86:983-8.

John, N., & Igor, S. (2015). Minimising second cancer risk following radiotherapy: current perspectives. *Cancer Manag. Res*, 7: 1-11.

Knoos, T., Wieslander, E., Cozzi, L., Brink, C., Fogliata, A., Albers, D., Nystrom H. & Lassen, S. (2006). Comparison of dose calculation algorithms for planning in external photon beam therapy for clinical situation. *Physics in Medicine and Biology*, Volume 51 number 22.

Kry, F., Salehpour, M., Followill, D., Stovall, M., Kuban, D. A., White, R. A., & Rosen, I. (2005). The calculated risk of fatal secondary malignancies form intensity-modulated radiation therapy. *Int J Radiat Oncol Biol Phys*, 62(4):1195-1203.

Kry, S., Salehpour, M., Titt, U., White, R., Stovall, M., & Followill, D. (2009). Monte Carlo study shows no significant difference in second cancer risk between 6 MV and 18 MV intensity-modulated radiation therapy. *Radiother Oncol*, 91(1):132-137. 10.1016/j.radonc.2008.11.020.

Laryea, D. O., Awuah, B., Amoah, Y. A., & Osei-Bonsu, E. (2014, 01 01). *Ghana incidence in Ghana,2012: evidence from a populated-based cancer*. Retrieved January 27, 2017, from Science.gov: https//www.science.gov

Leeuwen, V. F., & Travis, L. (2005). Risk of secondary malignancy in patients with selected primary cancers.In cancer:. *Principles & Practice of oncology, 7th ed; Devita, V.T., Hellman, S., Rosenberg, S.A., Eds.; Lippincott Williams & Wilkins: Philadelphia, PA, U.S.A*, 2575-2602.

Lilliscrap, S., Morgan, H., & Shakeshaft, J. (2000). X-ray leakage during radiotherapy. *Br J Radiat*, 73(871):793-794. Epub 2000/11/23.

Murray, L. J., Thompson M, C., Lilley, J., Cosgrove, V., Franks, K., & Sebag-Montefiore, D. (2015). Radiation-induced second primary cancer risks from modern external beam radiotherapy for prostate cancer: impact of Stereostatic Ablative Radiotherapy (SABR), Volumetric Modulated arc Therapy (VMAT) and Flattening Filter Free Radiotherapy. *Phys. Med. Biol.*, 60:1237-1257.

Murray, L., Henry, A., Hoskin, P., Siebert, F., & Venselaar, J. (2013). Second primary cancers after radiataion for prostate cancer: a review of data from planning studies. *Radiat Oncol*, 8:172. Epub 2013/07/10.

Murray, L., Henry, A., Hoskin, P., Siebert, F., & Venselaar, J. (2014). Second primary cancers after radiation for prostate cancer: a systematic review of the clinical data and impact of treatment technique. *Radiother Oncol*, 110:213-28. Eup 2014/02/04.

NCRNM, N. C. (2007). 2004-2006 cancer registration at National Center for Radiotherapy and Nuclear Medicine, Kumasi, Ghana. *Kumasi: KATH*.

NCRP, R. 1. (1993). Limitation of exposure to ionizing radiation.Bethseda, MD:. *National Council on Radiation Protection and Measurements*.

Neugut, A., Ahsan, H., Robinson, E., & Ennis, R. (1997). Bladder carcinoma and other second malgnancies after radiotherapy for prostate carcinoma. *Cancer*, 79: 1600-4.

Newhauser, W., & Durante, M. (2001). Assessing the risk of second malignancies after modern radiotherapy. *Nat. Rev. Cancer*, 11,438-448.

Podgorsak, E. (2005). *Radiation Oncology Physics: A Handbook for Teachers and students.* Vienna: International Atomic Energy Agency 1196; (ISBN:92-0-107304-6); 657.

registry, P.-b. c. (2014, 01 01). *National cancer registries*. Retrieved January 27, 2017, from Science.gov: https://www.science.gov

Ruben, J., Davis, S., Evans, C., Jones, P., Gagliardi, F., Haynes, M., & Hunter, A. (2008). The effect of intensity- modulated radiotherapy of radiation-induced second malignancies. *Int J Radiat Oncol Biol Phys*, 70(5):1530-1536. 10.1016/j.ijrobp.2007.08.046.

Scalzetti, E., Huda, W., Bhatt, S., & Ogden , K. (2008). A method to obtain mean organ dose in a Rando Phantom. *Health physics*, 95:241-244.

Schneider, U. (2006). Calculated risk of fatal secondary malignancies from intensity-modulated radiotherapy: in regard to Kry et al. *Int J Radiat Oncol Biol Phys*, 64(4):1.

Schneider, U. (2009). Mechanistic model of radiation-induced cancer after fractionated radiotherapy using linear quadratic formula. *Med. Phys.*

Schneider, U. (2011). Modeling the risk of secondary Malignancies after Raddiotherapy. *Genes*, ISSN 2073-4425. Retrieved from Genes.

Schneider, U., & Kaser-Hotz, B. (2005). A simple dose-response relationship for modelling secondary cancer incidence after radiotherapy. *Z Med Phys*, 15: 31-7.

Schneider, U., & Kaser-Hotz, B. (2005). Radiation risk estimates after radiotherapy: application of the organ equivalent dose concept to plateau dose-response relationships. *Radiat Environ Biophys*, 44:235-9.

Schneider, U., A, L., Besserer, J., Pemler, P., Lombriser, N., & Kaser-Hotz, B. (2007). The impact of dose escalation on secondary cancer risk of radiotherapy of prostate cancer. *Int J Radiat Oncol Biol Phys*, 68(3):892-897. 10.1016/j.ijrobp.2007.02.029.

Schneider, U., Lomax, M., Besserer, J., Permler, P., Lombriser, N., & Kaser-Hotz , B. (2007). The impact of dose escalation on secondary cancer risk after radiotherapy of prostate cancer. *Int J Radiat Oncol Biol Phys*, 68(3): 892-897. 10.1016/j.ijrobp.2007.04.014.

Schneider, U., Sumila, M., & Robotka, J. (2011). Site-specific dose response relationships for cancer induction from combined Japanese A-bomb and Hodgkins cohorts for doses relevant to radiotherapy. *Theor. Biol. Med. Model.*

Schneider, U., Sumila, M., & Robotka, J. (2011). Site-specific dose- response relationships for cancer induction from the combined Japanese A-bomb and Hodgkin cohorts for doses relevant to radiotherapy. *Theor. Biol. Med. Model*, 8:27.

Schneider, U., Zwahlen, D., Ross, D., & Kaser-Hotz, B. (2005). Estimation of radiation induced cancer from three-dimensional dose distributions: Concept of organ equivalent dose. *Int J Radiat Oncol BIol Phys*, 61(5):1510-5.

Sebestyen, Z. (2011). Developing advanced 3D conformal radiotherapy planning techniques for pancreas, prostate, cerebral and craniospinal irradiation. *PH.D Dissertation, University of Pecs.*, 15:84.

SEER, S. E. (2015, 01 01). *Science.gov*. Retrieved January 25, 2017, from National Cancer registry: https://www.science.gov

Singh, A., Kinoshita, Y., & Rovito, P. (2005). Higher than expected association of clinical prostate and bladder cancers. *J Urol*, 173:1526-9.

Sountoulides, P., Koletsas, N., Kikidakis, D., Paschalidis, K., & Sofikitis, N. (2010). Secondary malignancies following radiotherapy for prostate cancer. *Ther. Adv. Urol.*, 2(3) : 119-125 doi: 10.1177/1756287210374462.

Stathakis, S., Li, J., & Ma, C. (2007). Monte Carlo determination of radiation-induced cancer risk for prostate patients undergoing intensity-modulated radiation therapy. *J Appl Clin Med Phys*.

Stathakis, S., Roland , T., Papanikolaou, N., Li, J., & Ma, C. (2009). A prediction study on radiation-induced second malignancies for IMRT treatment delivery. *Technol Cancer Res Treat*, 8(2):141-148.

Stokkevag, C. H., Engeseth, G. M., Hysing, L. B., Ytre-Hauge, K. S., Ekanger, C., & Muren, L. P. (2015). Risk of radiation-induced secondary rectal and bladder cancer following radiatherapy of prostate cancer. *Acta Oncol*, 54: 1317-1325.

Stokkevag, C. H., Engeseth, G., Hysing, L., Ytre-Hauge, K., Ekanger, C., & Muren, L. (2015). Risk of radiation-induced secondary rectal and bladder following radiotherapy of prostate cancer. *Acta Oncologica*, 54:9, 1317-1325, DOI:10.3109/0284186X.20151061691.

Suit, H., Goldberg, S., Niemierko, A., Ancukiewicz, M., Hall, E., Goitein, M., . . . Paganetti, H. (2007). Secondary carcinogenesis in patients treated with radiation: A review of data on radiation-induced cancers in human, non-human primate, canine and rodent subjects. *Radiat. Res.*

Takam, R., Bezak, E., & Yeoh, E. (2009). Risk of second primary cancer follwoing prostate cancer raditherapy: DVH analysis using the competitive risk model. *Phys Med Biol*, 54(3):611-625. 10.1088/0031-9155/54/3/009.

Tanatar, B., & Yakinci, M. (2007). Malatya TURKEY Balkan Physics letters. *24th international Physics Congress of Turkish Physical Society* (pp. ISSN 1301-8329). Turkey: University Press.

UNSCEAR. (2000). Report to the General Assembly: Sources and effects of ionizing radiation Annex I. *Epidemiological evaluation of radiation-induced cancer*.

Upton, A. C. (1997). Radiobiological effects of low doses implications for radiobiological protection. *Radiat Res*, 71, 51-74.

Yoon, M., Ahn, S., Kim, J., Shin, D., Park, S., Lee, S., . . . Cho, K. (2010). Radiation induced cancers from modern radiotherapy techniques: intensity-modulated radiotherapy versus proton therapy. *Int J Radiat Biol Phys*, 77(5):1477-1485. 10.1016/j.ijrobp.2009.07.011.

APPENDIX

Table A. 1: Patients data on absorbed dose received by bladder and rectum during treatment.

Patient ID	Organ site	Age (yrs)	**Min dose/Gy**		**Max dose/Gy**		**Average dose/Gy**	
			Bladder	Rectum	Bladder	Rectum	Bladder	Rectum
1	Prostate	53	1.68	26.23	77.3	75.26	26.6	38.08
2	Prostate	72	3.49	2.74	79.51	79.37	44.29	47.39
3	Prostate	74	11.86	2.51	76.62	79.25	49.49	45.2
4	Prostate	65	8.98	7.65	77.99	77.11	52.54	49.71
5	Prostate	63	37.54	10.4	78.58	78.72	55.97	51.75
6	Prostate	68	21.45	2.71	78.69	77.81	57.8	35.85
7	Prostate	77	25.15	3.33	78.26	78.19	66.03	41.5
8	Prostate	78	0.82	2.16	79.23	78.05	25.48	38.48
9	Prostate	59	4.73	2.98	78.13	78.73	45.03	46.68
10	Prostate	78	2.05	2.32	79.82	77.95	40.28	46.1
11	Prostate	71	1.76	2.14	78.85	76.87	35.78	28.84
12	Prostate	61	1.89	1.98	78.49	78.11	37.55	30.62
13	Prostate	68	2.03	22.68	79.21	78.38	30.93	34.41
14	Prostate	68	28.22	12.3	82.84	82.57	62.89	57.86
15	Prostate	78	6.57	2.72	79.53	77.34	41.75	33.48
16	Prostate	73	3.03	3.56	80.77	78.6	43.13	48.42
17	Prostate	63	6.04	2.33	79.16	77.92	60.78	47.11
18	Prostate	62	46.45	7.15	77.88	76.95	55.87	50.97
19	Prostate	72	0.83	0.9	78.26	78.13	29.39	37.07
20	Prostate	78	2.52	22.63	79	79.36	37.66	54.36
21	Prostate	50	5.31	2.69	83.78	76.92	54.63	45.93
22	Prostate	73	2.63	2.28	79.46	78.01	32.34	39.14
23	Prostate	62	40.05	33.5	78.12	78.93	58.61	53.97
24	Prostate	79	3.31	3.88	80.76	77.22	47.6	46.25
25	Prostate	76	1.18	2.63	82.68	76.72	25.41	42.06
26	Prostate	70	13.09	20.24	79.56	76.88	52.13	53.43
27	Prostate	77	0.54	4.1	78.94	78.22	12.43	42.46
28	Prostate	71	4.36	3.05	78.67	77.98	49.9	45.25
29	Prostate	71	3.97	2.7	78.7	77.46	45.12	43.01
30	Prostate	73	2.63	2.28	79.46	78.01	32.34	39.14

Table A. 2: Dose calculation points for each patient in bladder and rectum

Patient ID	Age (yrs)	Bladder Dose Calculation Points (cGy)				Rectum Dose Calculation Points (cGy)			
		1	2	3	4	1	2	3	4
1	53	60.46	61.59	3.84	3.82	32.67	32.37	38.92	39.16
2	72	78.87	78.46	22.96	9.82	75.11	73.26	22.81	29.91
3	74	62.2	59.71	35.77	36.06	34.97	33.44	75.75	74.77
4	65	73.05	72	46.23	46.25	35.59	35.88	68.65	70.88
5	63	75.02	74.44	52.4	52.48	32.28	32.09	64.82	65.98
6	68	68.85	58.17	37.01	38.77	34.04	33.39	49.91	50.27
7	77	48.94	64.03	49.79	50.77	25.81	26.34	36.51	37.75
8	78	62.42	55.1	42.35	44.19	35.14	35.28	66.33	65.72
9	59	63.81	66.54	53.87	54.23	56.89	52.49	77.87	78
10	78	64.11	61.83	46.05	46.21	43.67	46.6	76.26	76.3
11	71	58.83	55.3	5.97	6.06	75.85	75.81	66.27	66.1
12	61	76.73	73.35	25.7	31.7	75.37	74.89	43.6	44.02
13	68	77.47	77.13	11.45	10.03	76.63	73.69	73.01	73.19
14	68	80.9	77.39	51.05	51.4	67.31	66.64	44.34	42.55
15	78	77.1	77.1	35.14	30.38	71.51	72.07	53.66	53.8
16	73	80.1	80.12	34.96	34.6	75.35	74.93	28.32	29.3
17	63	76.7	76.51	60.64	61.47	76.34	76.02	12.3	12.39
18	62	77.81	77.5	47.02	47.09	76.36	76.62	33.43	32.61
19	72	76.17	75.93	1.63	1.65	75.44	75.25	29.45	29.25
20	78	80.54	80.23	5.55	5.72	71.41	77.9	47.88	48.49
21	50	81.61	80.91	15.96	15.58	74.9	4.22	74.68	74.9
22	73	76.65	77	3.57	3.54	4.94	5.01	76.84	77.01
23	62	75.38	75.07	42.23	40.27	75.64	75.46	20.07	20.48
24	79	79.3	79.23	4.04	4.12	75.55	75.47	4.08	4.08
25	76	79.53	78.97	2.37	2.37	75.58	75.2	4.58	4.41
26	70	77.65	77.9	16.2	16.52	70.38	70.37	33	35.2
27	77	76.48	76.11	0.56	0.51	76.49	76.46	4.74	4.78
28	71	78.1	78.19	6.13	6.14	75.93	75.73	5.21	5.1
29	71	77.07	77.36	5.79	5.8	61.74	60.52	4.01	4.7
30	73	76.59	76.98	3.03	3.11	75.86	76.27	4.19	4.13

Table A. 3: Organ Equivalent Dose and Lifetime Attributable Risk using linear non-threshold model (figures 4.1 and 4.2)

Patient ID	OEDLNT(Bladder)	OEDLNT(Rectum)	LAR bladder	LAR Rectum
1	1.639408493	7.099206349	0.023935364	0.01171369
2	2.402805865	9.974702381	0.017660623	0.005984821
3	2.448685541	10.85962302	0.017997839	0.006515774
4	3.002148635	10.46626984	0.036025784	0.012559524
5	3.214610718	9.681051587	0.038575329	0.011617262
6	2.563195147	8.313988095	0.030758342	0.009976786
7	2.698811931	6.270337302	0.019836268	0.003762202
8	2.579120324	10.04315476	0.018956534	0.006025893
9	3.013776542	13.15724206	0.044001138	0.021709449
10	2.757836198	12.04513889	0.020270096	0.007227083
11	1.594539939	14.08878968	0.011719869	0.008453274
12	2.622345804	11.79960317	0.03146815	0.014159524
13	2.225480283	14.70833333	0.026705763	0.01765
14	3.295500506	10.95436508	0.039546006	0.013145238
15	2.777047523	12.45238095	0.020411299	0.007471429
16	2.904196158	10.3125	0.021345842	0.0061875
17	3.479777553	8.782242063	0.041757331	0.01053869
18	3.152426694	10.8640873	0.03782912	0.013036905
19	1.963852376	10.38640873	0.014434315	0.006231845
20	2.174418605	12.18650794	0.015981977	0.007311905
21	2.45273003	11.34424603	0.035809858	0.018718006
22	2.031850354	8.125	0.0149341	0.004875
23	2.944261881	9.506448413	0.035331143	0.011407738
24	2.106799798	7.895833333	0.015484979	0.0047375
25	2.063195147	7.925099206	0.015164484	0.00475506
26	2.379550051	10.36458333	0.017489693	0.00621875
27	1.942113246	8.059027778	0.014274532	0.004835417
28	2.130434783	8.03422619	0.015658696	0.004820536
29	2.098331648	6.496527778	0.015422738	0.003897917
30	2.018579373	7.958829365	0.014836558	0.004775298

Table A. 4: Organ Equivalent Dose and Lifetime Attributable Risk using linear-plateau model (figures 4.5 and 4.6)

Patient ID	OED (Lin-plat.) Bladder	OED (Lin-plat.) Rectum	LAR Bladder	LAR Rectum
1	0.196078431	3.845669169	0.002862745	0.006345354
2	0.196078431	3.843195835	0.001441176	0.002305918
3	0.196078431	3.84588455	0.001441176	0.002307531
4	0.196078431	3.845976306	0.002352941	0.004615172
5	0.196078431	3.845707175	0.002352941	0.004614849
6	0.196078431	3.845848597	0.002352941	0.004615018
7	0.196078431	3.843837385	0.001441176	0.002306302
8	0.196078431	3.845950413	0.001441176	0.00230757
9	0.196078431	3.846152343	0.002862745	0.006346151
10	0.196078431	3.846137311	0.001441176	0.006346127
11	0.196078431	3.846153776	0.001441176	0.002307692
12	0.196078431	3.846132074	0.002352941	0.004615358
13	0.196078431	3.846153829	0.002352941	0.004615385
14	0.196078431	3.846129247	0.002352941	0.004615355
15	0.196078431	3.846152183	0.001441176	0.002307691
16	0.196078431	3.845071446	0.001441176	0.002307043
17	0.196078431	3.76851637	0.002352941	0.00452222
18	0.196078431	3.84579247	0.002352941	0.004614951
19	0.196055548	3.845220495	0.001441008	0.002307132
20	0.196078431	3.846146846	0.001441176	0.002307688
21	0.196078431	3.525188039	0.002862745	0.00581656
22	0.19607843	3.318614655	0.001441176	0.001991169
23	0.196078431	3.836263075	0.002352941	0.004603516
24	0.196078431	3.180425463	0.001441176	0.001908255
25	0.196077879	3.248371964	0.001441172	0.001949023
26	0.196078431	3.845871293	0.001441176	0.002307523
27	0.189622665	3.288300965	0.001393727	0.001972981
28	0.196078431	3.34270405	0.001441176	0.002005622
29	0.196078431	3.223867843	0.001441176	0.001934321
30	0.196078416	3.194109762	0.001441176	0.001916466

Table A. 5: Organ Equivalent Dose and lifetime Attributable Risk using competition model (figures 4.9 and 4.10)

Patient ID	OED(com) Bladder	OED(com) Rectum	LAR Bladder	LAR Rectum
1	1.096754866	0.011206255	0.016012621	1.84903E-05
2	0.496624873	0.06345456	0.003650193	3.80727E-05
3	0.004405523	0.006229767	3.23806E-05	3.73786E-06
4	0.000258918	0.003983112	3.10701E-06	4.77973E-06
5	4.14439E-05	0.01057605	4.97327E-07	1.26913E-05
6	0.002690488	0.007055967	3.22859E-05	8.46716E-06
7	0.000139536	0.053094938	1.02559E-06	3.1857E-05
8	0.000631665	0.004613616	4.64274E-06	2.76817E-06
9	2.61894E-05	1.33134E-05	3.82365E-07	2.19672E-08
10	0.000268859	0.000265298	1.97611E-06	1.59179E-07
11	1.168378946	1.66922E-07	0.008587585	1.00153E-10
12	0.032756488	0.00036419	0.000393078	4.37028E-07
13	0.808313931	1.70842E-08	0.009699767	2.0501E-11
14	5.98269E-05	0.000422142	7.17922E-07	5.06571E-07
15	0.011523945	1.43493E-05	8.4701E-05	8.60956E-09
16	0.005903403	0.025717	4.339E-05	1.54302E-05
17	2.83698E-06	0.773998133	3.40437E-08	0.000928798
18	0.000204548	0.008488702	2.45458E-06	1.01864E-05
19	0.661676998	0.022252438	0.004863326	1.33515E-05
20	1.174060852	9.11376E-05	0.008629347	5.46826E-08
21	0.384688505	0.6408123	0.005616452	0.00105734
22	1.065810422	1.338171535	0.007833707	0.000802903
23	0.001092423	0.186848285	1.31091E-05	0.000224218
24	1.119844589	1.266302148	0.008230858	0.000759781
25	0.858204256	1.306899611	0.006307801	0.00078414
26	0.347433582	0.006555353	0.002553637	3.93321E-06
27	0.250606333	1.326342084	0.001841957	0.000795805
28	1.165327028	1.345618757	0.008565154	0.000807371
29	1.172534082	1.290251267	0.008618125	0.000774151
30	0.996108271	1.275216811	0.007321396	0.00076513

Table A. 6: LAR relationship in bladder and rectum using LNT model (figure 4.3)

Patient ID	%LAR Bladder	%LAR Rectum
1	1.171986855	0.376220238
2	1.427453236	0.389791667
3	1.443431496	0.47375
4	1.483655839	0.475505952
5	1.49341001	0.477529762
6	1.516448433	0.482053571
7	1.542273761	0.483541667
8	1.548497851	0.4875
9	1.565869565	0.598482143
10	1.598197674	0.602589286
11	1.748969287	0.61875
12	1.76606231	0.621875
13	1.799783873	0.623184524
14	1.895653438	0.651577381
15	1.983626769	0.722708333
16	2.027009606	0.731190476
17	2.041129929	0.747142857
18	2.134584176	0.845327381
19	2.3935364	0.997678571
20	2.67057634	1.053869048
21	3.075834176	1.14077381
22	3.146814965	1.16172619
23	3.533114257	1.171369048
24	3.580985844	1.255952381
25	3.602578362	1.303690476
26	3.782912032	1.31452381
27	3.857532861	1.415952381
28	3.954600607	1.765
29	4.175733064	1.871800595
30	4.400113751	2.17094494

Table A. 7: Summary of mean lifetime risk of radiation induced-related cancer for LNT model (figure 4.4)

Age group at exposure (yrs.)			
Organ	50-60	61-70	71-80
% Bladder	3.458211999	3.354866595	1.6728868
% Rectum	1.738038194	1.203104167	0.5756968

Table A. 8: LAR relationship in bladder and rectum using linear-plateau model (figure 4.7)

Patient ID	%LAR Bladder	%LAR Rectum
1	0.139372659	0.190825528
2	0.144100828	0.191646586
3	0.144117241	0.193432071
4	0.144117635	0.194902318
5	0.144117646	0.197298058
6	0.144117647	0.199116879
7	0.144117647	0.200562243
8	0.144117647	0.23059175
9	0.144117647	0.230630243
10	0.144117647	0.230704287
11	0.144117647	0.23071323
12	0.144117647	0.230752278
13	0.144117647	0.230753073
14	0.144117647	0.230757025
15	0.144117647	0.230768811
16	0.144117647	0.230769131
17	0.144117647	0.230769227
18	0.144117647	0.452221964
19	0.235294118	0.460351569
20	0.235294118	0.461484861
21	0.235294118	0.461495096
22	0.235294118	0.461501832
23	0.235294118	0.461517157
24	0.235294118	0.46153551
25	0.235294118	0.461535849
26	0.235294118	0.461538459
27	0.235294118	0.581656026
28	0.286274509	0.634535413
29	0.28627451	0.634612656
30	0.28627451	0.634615137

Table A. 9: Summary of mean lifetime risk at exposure based on age group for linear-plateau model (figure 4.8)

Age group at exposure (yrs.)			
Organ	50-60	60-70	71-80
% Bladder	0.28627451	0.226176471	0.143872861
% Rectum	6.169353964	4.425853837	2.646639147

Table A. 10: LAR relationship for each patient using competition model (figure 4.11)

Patient ID	%LAR Bladder	%LAR Rectum
1	3.40437E-06	2.0501E-09
2	3.82365E-05	1.00153E-08
3	4.97327E-05	8.60956E-07
4	7.17922E-05	2.19672E-06
5	0.000102559	5.46826E-06
6	0.000197611	1.59179E-05
7	0.000245458	4.37028E-05
8	0.000310701	5.06571E-05
9	0.000464274	0.000276817
10	0.001310907	0.000373786
11	0.003228585	0.000393321
12	0.003238059	0.000477973
13	0.004339001	0.000846716
14	0.0084701	0.001018644
15	0.039307785	0.001269126
16	0.184195655	0.001335146
17	0.255363683	0.00154302
18	0.365019282	0.001849032
19	0.486332594	0.003185696
20	0.561645218	0.003807274
21	0.630780128	0.022421794
22	0.732139579	0.075978129
23	0.78337066	0.076513009
24	0.823085773	0.077415076
25	0.856515366	0.078413977
26	0.858758525	0.079580525
27	0.86181255	0.080290292
28	0.862934726	0.080737125
29	0.969976717	0.092879776
30	1.601262104	0.10573403

Table A. 11: Summary of mean lifetime risk according to age at irradiation for competition model (figure 4.12)

Age group at exposure (yrs.)			
Organ	50-60	61-70	71-80
% Bladder	0.7209819	0.1269869	0.4389268
% Rectum	0.0358618	0.0119402	0.0329101